Università di Foggia

UNIVERSITÀ DEGLI STUDI DI FOGGIA

FACOLTÁ DI MEDICINA E CHIRURGIA

PhD Course in Experimental and Regenerative Medicine
XXXI Cycle

Dissecting the TRIM8 role in the pathogenesis of glioma

Tutor
Prof. V.M Fazio

PhD Student
Santina Venuto

Supervisor
Dr. Giuseppe Merla

A.A. 2017/2018

ABSTRACT

Human gliomas are a heterogeneous group of primary malignant brain tumors, whose molecular pathogenesis is not yet solved. Therefore, understanding the molecular mechanisms underlying their aggressive behavior may lead to better management, appropriate therapies, and good outcomes through the identification of novel specific glioma-associated genes. Members of the tripartite motif (TRIM) proteins family are involved in many biological processes, including transcriptional regulation, cell proliferation and differentiation and cell cycle progression. Alterations of TRIM proteins are associated with a variety of pathologies like developmental disorders, inflammatory diseases and cancers. Among TRIMs protein family, TRIM8 encodes an E3 ubiquitin ligase involved in various pathological processes, including hypertrophy, antiviral defense, encephalopathy, and cancer development. We have identified TRIM8 as a gene aberrantly expressed in gliomas, whose expression correlates with unfavorable clinical outcome in glioma patients. To gain insights into the TRIM8 functions, we profiled the TRIM8 transcriptome and interactome in primary mouse embryonic neural stem cells using RNA-sequencing and proteomics, followed by bioinformatics analysis. Functional analysis, including biochemical and cellular assays were then performed to explore TRIM8 roles in different pathways.

Our study firstly identified enriched pathways related to the neurotransmission and to the central nervous system (CNS) functions, providing additional evidence about the existence of a functional interactive crosstalk between TRIM8 and STAT3 with possible implications in the development and progression of glioma. Then, we found that TRIM8 interacts with KIFC1 and KIF11/Eg5, two master regulators of mitotic spindle assembly and cytoskeleton reorganization. Exploring the TRIM8 role in the mitotic spindle machinery, we showed that TRIM8 localizes at the mitotic spindle during mitosis and plays a role in centrosome separation at the beginning of mitosis with a subsequent delay of the mitotic progression and impact on chromosomal stability.

Our results substantiate the role of TRIM8 in the brain functions through the deregulation of genes involved in different CNS-related pathways, including JAK-STAT. Moreover, we provided insights on the physiological function of TRIM8 in the mitotic spindle machinery, pointing to an emerging role for TRIM8 in the regulation of mitosis.

1. Introduction

1.1. General features of glioblastoma

Gliomas are the most universal inherent brain tumors in adults and are nearly uniformly fatal. Glioblastoma (GBM) is the most common and the most malignant variant in the wide spectrum of intrinsic glial brain tumors being the most aggressive diffuse glioma of astrocytic lineage. Defining histopathological features are necrosis and endothelial proliferation, resulting in the assignment of grade IV glioma, the highest grade in the World Health Organization (WHO) classification of brain tumors[1].

GBMs are further classified into primary (*de novo*) and secondary tumors that arise from different frequently altered pathways[2]. Primary GBM occurs *de novo* without evidence of a less malignant precursor, whereas secondary GBM develops from initially low-grade diffuse astrocytoma (WHO grade II diffuse astrocytoma) or anaplastic astrocytoma (Grade III). GBM develops via a complex network of different genetic and molecular aberrations, leading to significant changes in major signaling pathways. Gene deregulation shows a crucial role in advancement of gliomas and glioblastoma[3].

While there have been advances in forgiving the molecular genetics of these tumors, the cell type(s) of origin are still uncertain, and the molecular determinants of disease aggressiveness are not well understood[3]. Therefore, it is essential to explore the prognostic factors of gliomas and glioblastoma and further to study the molecular mechanism responsible for gliomas and glioblastoma progression.

1.2. TRIM proteins superfamily

Members of the tripartite motif (TRIM) protein family (also known as RBCC family) contain a tripartite motif domain. The TRIM is composed of three zinc-binding domains, a RING (R), B-box type 1 (B1) and B-box type 2 (B2), followed by a coiled-coil (CC) region[4, 5]. Proteins belonging to this family are implicated in a variety of processes like development and cell growth and are involved in several human diseases[6].

The overall architecture of the tripartite motif is highly conserved throughout evolution and serves as an integrated functional structure. The RING is a DNA-binding domain with a zinc finger motif and mainly functions as an ubiquitin-protein isopeptide ligase (E3)[4, 7, 8]. The B-Box1 (B1) and B-Box-2 (B2) domains are critical determinants of the TRIM motif, influencing the substrate recognition and/or the ubiquitin ligase activity and determining the ability of TRIM proteins to form homo-multimers and interact with other proteins. They have different length and consensi and, when found together, the type 2 B-box is always preceded by the type 1[8, 9]. A predicted coiled-coil (CC) region invariably follows B1 and B2 and is involved in the formation of high molecular weight complexes and in the definition of discrete subcellular compartments within the cell[6, 8].

Finally, one or more C-terminal domains of different length and nature usually follow the TRIM motif to confer specificity of functions to the entire protein[6, 8] (Fig. 1).

TRIM proteins identify a variety of cellular compartments, specifically depending on the integrity of their domains and their propensity to form high-order molecular weight structures. The propensity of these proteins to define specific and often novel cellular compartments and to facilitate protein aggregation suggests that they might act as a protein scaffold for the assembly of higher order molecular weight structures to recruit proteins involved in several distinct processes[8].

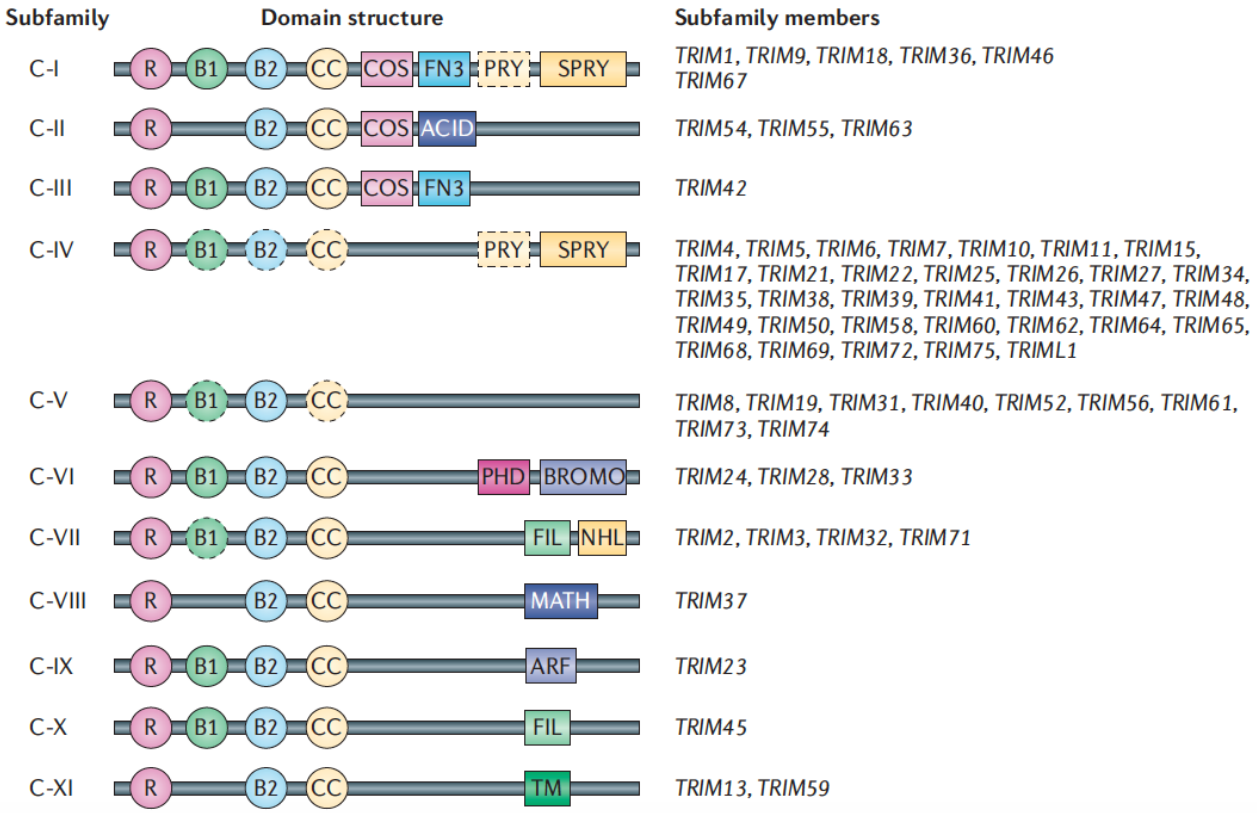

Figure 1. The structural classification of human tripartite motif (TRIM) subfamily (C-I to C-XI). Almost all TRIM proteins have a RING-finger domain (R), one or two B-box domains (B) and a coiled-coil domain (CC). Some members of the subfamily lack one or more amino-terminal domains (shown as dashed outline domains). ACID, acid-rich region; ARF, ADP-ribosylation factor family domain; BROMO, bromodomain; COS, cos-box; FIL, filamin-type I G domain; FN3, fibronection type III repeat; MATH, meprin and TRAF-homology domain; NHL, NCL1, HT2A and LIN41 domain; PHD, PHD domain; PRY, PRY domain; SPRY, SPRY domain; TM, transmembrane region; Ub, ubiquitin.

1.3. TRIM/RBCC as a class of E3-Ubiquitin ligases

Although the TRIM/RBCC family proteins have a highly conserved structure, they are involved in a variety of cellular processes, including regulation of cell cycle progression, intracellular signaling, differentiation, development, apoptosis, protein quality control, innate immunity, autophagy, and carcinogenesis[10]. The presence of the RING domain and its strong association to ubiquitination suggests a role for this protein family in the ubiquitination process[11].

Ubiquitination is a versatile post-translational modification mechanism used by eukaryotic cells mainly to control protein levels through proteasome-mediated proteolysis, playing an important role in the degradation of proteins that function in the cell cycle, intracellular signaling, DNA repair, protein quality control, and transcriptional regulation[12]. Protein ubiquitination is a multi-step process that involves at least three classes of enzymes. The E1 ubiquitin-activating enzyme activates ubiquitin with ATP. The E2 ubiquitin-conjugating enzyme has a core catalytic domain required for transferring ubiquitin from E1 to E2 itself. In the last step, the E3 ubiquitin ligase enzyme recognizes specific substrate protein and conjugates ubiquitin to a lysine on a specific target protein. The resulting polyubiquitinated conjugates are detected and rapidly degraded by the 26S proteasome, a protein complex for protein degradation with nuclear and cytoplasmic functions[10] (Fig. 2). The ubiquitin proteasome system (UPS) handles 80 to 90% of intracellular protein degradation, including key signaling molecules that promote cell cycle progression, cellular adhesion, and proliferation and induce anti-apoptotic pathways[13]. Interestingly, deregulated proteolysis of oncoproteins and tumor suppressors involved in major signaling cancer pathways can contribute to the development of different tumors, including glioma[13, 14].

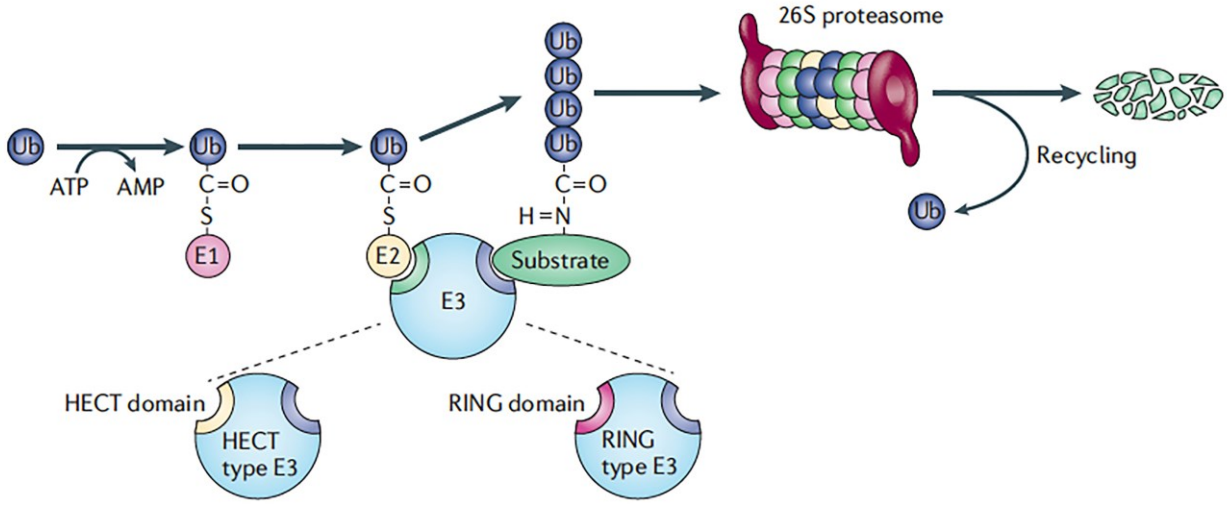

Figure 2. An overview of the ubiquitin-proteasome system. Ubiquitin conjugation is catalyzed by ubiquitin-activating enzyme (E1), ubiquitin-conjugating enzyme (E2) and ubiquitin ligase (E3). E3 is a scaffold protein that mediates between E2 and the substrate, and it is thought to be the component of the ubiquitin conjugation system that is most directly responsible for substrate recognition. The resulting covalent ubiquitin ligations form polyubiquitylated conjugates that are rapidly detected and degraded by the 26S proteasome. On the basis of occurrence of covalent linkage with ubiquitin, E3 enzymes have been classified into two families: the HECT family and the RING family.

It is generally accepted that E3 ligases are responsible for substrate recognition and therefore confer specificity to the system[15]. Over 600 E3 ligases have been characterized in humans and are classified into 3 different classes: homologous to E6-AP carboxyl terminus (HECT), really interesting new gene (RING) and RING-between-RING (RBR)[16]. RING proteins are the largest

class of E3 ligases and among them the tripartite motif (TRIM) family proteins represent the largest subfamily of RINGs[17]. To date, there are more than 80 known TRIM protein genes in humans[10] involved in many biological processes, and their alteration are associated with a variety of pathologies including developmental disorders, inflammatory diseases and cancers[17].

1.3.1. TRIM proteins are involved in tumor development and progression

Ubiquitylation is one of the many post-translational modifications used by eukaryotic cells to regulate cellular physiology, and the ubiquitin-mediated proteolytic pathway has a crucial role in the elimination of short-lived regulatory proteins, including oncogenes and tumor suppressor genes[18, 19]. As TRIM proteins are involved in several biological processes, some members of the tripartite motif protein family are thought to be important regulators of carcinogenesis[18]. Indeed, changes in the expression of some TRIM proteins are strongly correlated with the malignancy of cancers and prognosis[10].

Relevant for this study, a number of TRIMs are involved in glioma development and progression with both oncogenic and tumor suppressor role. Briefly, TRIM37 has an oncogenic role in glioma progression influencing proliferation, migration/invasion, and the epithelial-mesenchymal transition (EMT) phenotype in glioma cells, through the regulation of PI3K/Akt pathway[20, 21]. TRIM24 expression is positively correlated with glioma malignancy and is required as EGFR co-activator, recruiting and stabilizing STAT3 oncogene in multiple glioma cell lines[22, 23]. Moreover, TRIM28 is over expressed in glioma and its expression positively correlates with tumor malignancy, poor overall survival and progression-free survival[24, 25]. Finally, TRIM11 expression levels are upregulated in human high-grade gliomas and glioma-derived stem-like cells (GSCs). TRIM11 overexpression potentially leads to a more aggressive glioma phenotype, mediated through the EGFR signaling pathway[26]. On the other hand, TRIMs like TRIM3 and TRIM11 have a tumor suppressor role in glioma. In particular, TRIM3 is deleted in primary human glioma[27] while TRIM45 interacts with and stabilizes p53 in glioma, promoting the K63-linked ubiquitination of p53 to protect p53 from degradation and inactivation, thereby suppressing GBM proliferation and tumorigenicity[28].

1.4. TRIM proteins control cell cycle progression

Among the cellular processes TRIMs are involved in, one that have to be faithful coordinated and regulated is the control of cell cycle and in particular of mitosis[29]. Cell cycle control at different checkpoints between S and M phases is responsible for cells progression and proliferation and many TRIM proteins are involved in controlling cell cycle transition phases. To obtain an optimal cell cycle progression and cells proliferation, TRIMs regulate proteins involved in the cell cycle progression like cyclins and cyclin-dependent kinases (CDKs)[30].

TRIM proteins can control above all, the regulation of the different mitotic phases. Interestingly, TRIM superfamily has been shown to possess a domain necessary for the microtubule binding[31]. As a consequence, a lot of TRIM proteins co-localize with or are important for the regulation of many key components of the mitotic spindle, including kinetochore, centrosomes and midbodies[32-37].

1.4.1. Kinesin motor proteins control mitotic spindle formation

The mitotic spindle is a dynamic bipolar structure that self-assembles from component parts at the entry into mitosis. The two ends of the spindle are called spindle poles, are located where spindle microtubules converge and are associated with centrosomes, the sites for microtubule nucleation. Correct spindle formation and function by generating forces that establish and maintain spindle bipolarity and elongation, requires various motor microtubule associated proteins (MAPs) that regulate the nucleation, organization, dynamics, and crosslinking of spindle microtubules. Among motor proteins, Kinesin-5 family members function as bipolar homotetramers, with pairs of motor heads at opposite ends of an elongated molecule. This structural organization allows the motor to crosslink two adjacent microtubules. Among kinesin-5 family proteins, KIF11/Eg5 is a plus-end directed microtubule motor protein that forms a bridge between two adjacent and antiparallel microtubules to facilitate their movement in opposite directions from each of the duplicated centrosomes relative to one another, driving bipolar spindle formation[38, 39]. KIF11/Eg5 interacts with microtubules and moves toward plus ends with short run lengths in an ATP-dependent, bidirectional diffusive behavior of the protein N-terminus[40].

In contrast to plus-end-directed kinesins, kinesin-14 family proteins are specific minus-end-directed motors; they utilize the chemical energy of ATP hydrolysis to move along microtubules from their plus- to their minus-end, exploiting ATP hydrolysis[41, 42]. Among the three members of this family, KIFC1 (HSET) is a dimer involved in spindle pole organization[43].

The bipolar spindle apparatus is maintained by antagonistic relationships[41]. Within the bipolar spindle, on parallel and anti-parallel microtubules, there is an antagonistic relationship between KIFC1 and KIF11 in order to crosslink and slide microtubules, a common mechanism to maintain correct spindle organization[44-46]. Briefly, kinesin-14 motors generate inward pulling forces on spindles, whereas the kinesin-5 motors have been shown to generate outwards forces on spindles[47]. Exerting opposite forces, KIFC1 and KIF11 cooperatively regulate microtubule aster formation, centrosome separation and correct spindle organization, thus the balance between KIFC1 and KIF11 is responsible for correct microtubule assembly[41] (Fig. 3). Remarkably, disturbing the stoichiometric balance between KIFC1 and its counterforce generating kinesin KIF11 is responsible of the formation of monopolar and multipolar spindles observed in different forms of cancers[38, 48].

In particular, monopolar spindles occur when only a single spindle pole and a single microtubule aster are present in a prometaphase cell[49].

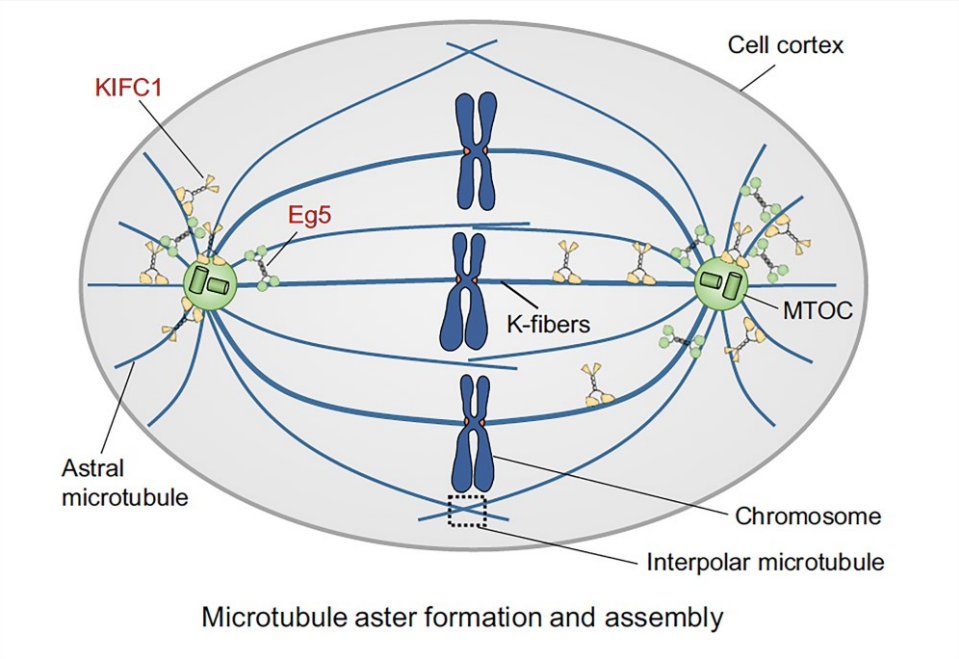

Figure 3. Counterbalance between KIFC1 and KIF11/Eg5 motors. In mammalian, kinesin-14 KIFC1 and kinesin-5 Eg5 cooperatively regulate microtubule aster formation, centrosome separation and spindle assembly.

1.5. TRIM8

The TRI-partite Motif 8 (TRIM8)/GERP protein is a member of the TRIM family proteins[6]. TRIM8 protein is composed of 551 amino acids (aa) with a molecular weight of 61.5 kDa. TRIM8 protein also contains Nuclear Localization Signals (NLS), thus it is a nuclear protein localized to structures best described as "nuclear bodies". These nuclear structures depend on the coiled-coil domain, since the deletion of this domain induces diffused nuclear staining and no discrete foci[50] (Fig. 4). Interestingly, TRIM8 modulates the activity of important cellular proteins through protein-protein interactions mainly mediated by the coiled-coil and the C-terminus domain[51].

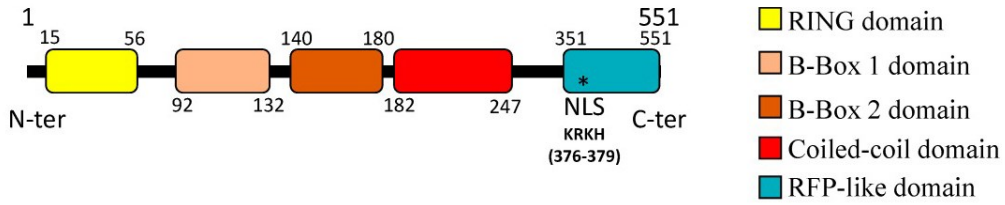

Figure 4. TRIM8 protein structure. The different TRIM8 domains are reported with the numbers indicating the first and the last amino acid for each one.

TRIM8 gene maps on chromosome 10q24.3, within a region mostly involved in deletion or rearrangements in glioblastoma and has therefore been designated as glioblastoma expressed RING

finger protein (GERP)[52]. We described *TRIM8* as a brain gene whose expression correlates with unfavorable clinical outcome in glioma patients. We found that a restored TRIM8 expression induced a significant reduction of clonogenic potential in U87MG and patient's glioblastoma cells. Finally, we provide experimental evidences showing that miR-17 directly targets the 3' UTR of *TRIM8* and post-transcriptionally represses *TRIM8* expression[53].

1.5.1. The tumor suppressor role of TRIM8

TRIM8 shows a dual role either as oncogene or as tumor suppressor gene, depending on the cellular context in quite diverse pathways, as embryonic development and differentiation, innate immune response and in a variety of human cancers[50]. Involvement of TRIM8 in cancer was first highlighted in brain tumors including glioblastomas, where the TRIM8 loss of heterozygosity was observed[52]. Moreover, TRIM8 tumor suppressor role was also found in other tumors as glioblastoma multiforme (GBM), larynx squamous cell carcinoma (LSCC), clear cells renal carcinoma (ccRCC), anaplastic thyroid cancer (ATC), colorectal cancer (CRC), chronic lymphocytic leukemia (CLL) and osteosarcoma cell lines[50] (Fig. 5).

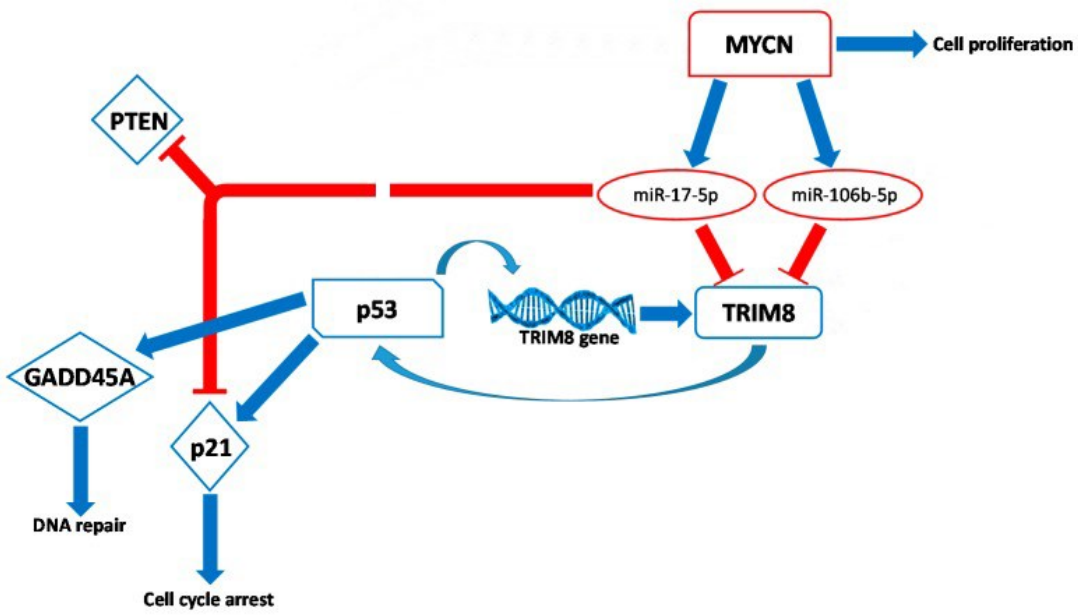

Figure 5. Schematic representation of the tumor suppressor network involving TRIM8. Following cellular stress, the p53 tumor suppressor protein trans activates TRIM8 gene, which in turn stabilizes p53, promoting the transcription of p53 target genes involved in cell proliferation arrest (p21), DNA repair (GADD45A), and the suppression of the MYCN oncogenic activity. MYCN promotes the transcription of miR-17-5p and miR-106b-5p, which target TRIM8 mRNA, promoting its degradation.

- TRIM8 in the regulation of p53

Experimental evidences has outlined *TRIM8* as one of the gene which low expression levels correlates with nodal metastatic progression in primary larynx squamous cell carcinoma (LSCC)

and whose stable expression inhibits tumor cell colony formation *in vitro* and tumor cell growth[51]. In different types of cancer, TRIM8 is implicated in a feedback loop in the tumor suppressor circuit controlled by p53[54, 55]. Tumors harboring *p53* mutations, which lead to expression of inactive p53 protein, account for about 50% of all human cancers and predict a considerably worse patient prognosis in comparison with malignancies with functional p53[55]. Besides the many tumors that have an inactivating mutation in the p53 coding sequence, an additional 40% contain a wild-type *p53* gene but the p53 pathway is often inactivated through alterations in its regulators or rather still unknown mechanisms[55].

In human osteosarcoma cell lines, TRIM8 directs the cells toward a program of cell cycle arrest, modulating p53 stability and activity[54]. In particular, TRIM8 physically interacts with p53, stabilizes and activates p53 protein enhancing its half-life, resulting in a suppression of cell proliferation, due to a p53-dependent cell cycle arrest in G1. This TRIM8-mediated p53 stabilization occurs through MDM2, without a directly interaction between TRIM8 and MDM2, but resulting in a highly impairment of MDM2-p53 interaction. Under stress conditions p53 induces TRIM8 expression, which in turn stabilizes p53, leading to cell cycle arrest and reduction of cell proliferation through the enhancement of p21 and GADD45 expression, two p53 targets[54] (Fig. 5). A prominent role for TRIM8 as tumor suppressor implicated in the p53 loop was shown in clear cell Renal Cell Carcinoma (ccRCC). *TRIM8* is down regulated in patients affected by ccRCC, the most common and aggressive subtype of RCC and the decrease of TRIM8 expression is linked to a malignant transformation of the cells. In this cancer, TRIM8 down regulation suppresses p53 activity increasing cell proliferation rate, as a result of MDM2 protein stabilization and p53 protein degradation. Interestingly, the restoration of TRIM8 levels in RCC cell line makes them more sensitive to the action of chemotherapy, through the reactivation of the p53 pathway, making TRIM8 an enhancer of the chemotherapy efficacy[55].

1.5.2. The oncogenic role of TRIM8

Although some studies point to the tumor suppressor role of TRIM8, a number of oncogenic mechanisms have been proposed concerning a TRIM8 role in the regulation of inflammatory pathways, including the NF-kB pathway, and therefore supporting tumor onset and progression[50] (Fig. 6).

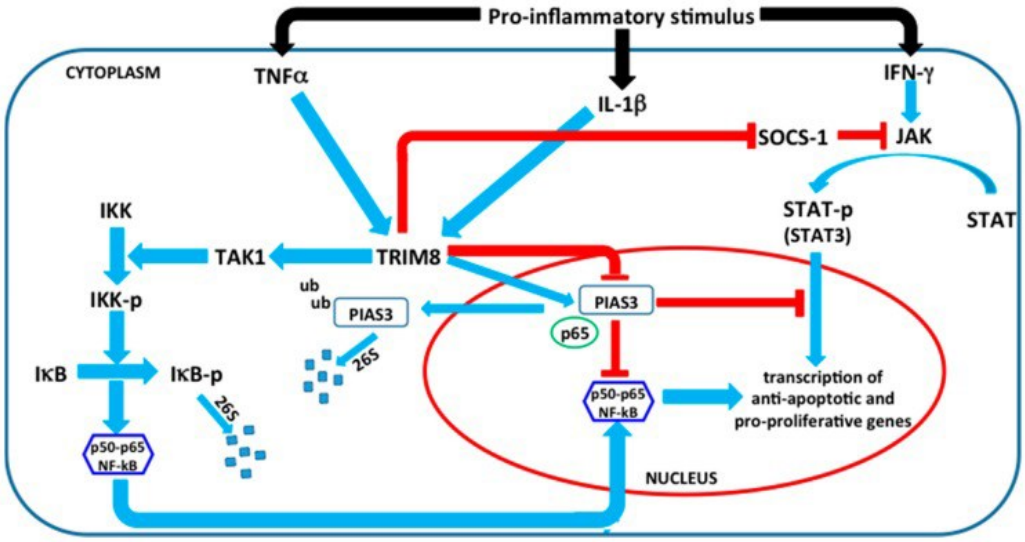

Figure 6. Schematic representation of the oncogenic network involving TRIM8. Proinflammatory cytokines, such as TNFα and IL-1β, promote NF-κB activation mediated by TRIM8, through two different mechanisms: i) promoting the translocation of PIAS3 from the nucleus to cytoplasm and its subsequent degradation; PIAS3 in the nucleus interacts with p65, preventing NF-κB activation; ii) mediating TAK1 polyubiquitination and subsequent activation. TAK1 is a member of the MAPK kinase family that promotes the phosphorylation of IKK (IκB Kinase) leading to the phosphorylation of IκBα, its degradation, and activation of NF-κB. Moreover, TRIM8 induces the activation of the JAK-STAT pathway promoted by Interferon-γ (IFN-γ), through the degradation of two STAT proteins inhibitors, PIAS3 and SOCS-1 (suppressor of cytokine signalling-1).

-TRIM8 has an oncogenic role in TNFα/NF-kB pathway

NF-kB is an inducible transcription factor and its activation plays a pivotal role in many cellular events such as cell proliferation, inhibition of apoptosis, and innate immunity[56]. The deregulation of this pathway has been observed in many cancers, skeletal abnormalities, neurodegenerative and autoimmune diseases and metabolic disorders[57]. NF-kB activation is induced by tumor necrosis factor alpha (TNFα) and IL-1β and requires the signal-induced phosphorylation and degradation of IκB proteins that is mediated by IκB kinase (IKK) complex[58]. Interestingly, also ubiquitination has a role in the regulation of NF-kB pathway. The binding of TNFα to its receptor leads to the recruitment of several ubiquitin ligases that are either auto-ubiquitinated or ubiquitinates other substrates to activate downstream IKK complex, resulting in the translocation of NF-kB to the nucleus and consequent activation[59-61]. In particular, TRIM8 exerts an oncogenic role in this context, positively regulating TNF-induced NF-κB activation in two ways: i) promoting TGFβ activated kinase 1 (TAK1) activation; ii) through the translocation of protein inhibitor of activated STATs 3 (PIAS3) from nucleus to cytoplasm[62, 63].

TRIM8 interacts with TAK1, a serine/threonine kinase essential for TNFα- and IL-β–induced NF-κB activation. TAK1, together with other proteins, activates the IKK complex after a large variety of stimuli, including the proinflammatory cytokines tumor necrosis factor α (TNFα) and

interleukin-1β (IL-1β)[64]. Interestingly, TAK1 polyubiquitination is involved in the regulation of TAK1-mediated signaling pathways[65]. In this context, TNFα and IL-1β trig TRIM8 mediated K63-linked polyubiquitination of TAK1 at residue K158, thus stimulating TNFα- and IL-1β–induced NF-κB activation[62, 66].

Another way by which TRIM8 positively regulates TNF induced NF-kB activation is at p65 level, stimulating the translocation of PIAS3 from nucleus to cytoplasm. PIAS3 negatively regulates NF-kB transcription via its interaction with p65 in the nucleus[67]. Mediating the spatial regulation and turnover of PIAS3, TRIM8, activated and stabilized by TNFα, inhibits PIAS3-mediated negatively regulation of NF-kB (Fig. 6)[63].

TNF is one of the pro-inflammatory cytokines that is constitutively present in tumor microenvironments and regulates various steps of tumorigenesis[68]. TRIM8 positive regulation of TNF-mediated NF-kB activation supports TRIM8 oncogenic role. This observation is enforced by the evidence that TRIM8 regulates clonogenic and migration ability of cells, through NF-kB pathway[63].

-TRIM8 regulates the suppressor of cytokine signaling-1 (SOCS-1)

Another example in which TRIM8 has been described as an oncogene concerns its role in decreasing the protein stability of SOCS-1 and reversing the SOCS-1-mediated inhibition of JAK-STAT activation by IFNγ[69]. Cytokines control many different cellular functions, including proliferation, differentiation, and gene expression and the biological cellular response to cytokines involves a complex network of signal transduction machinery[70]. Oligomerization of cytokine receptors expressed on the surface of target cells triggers the activation of members of the JAK family of protein-tyrosine kinases that constitutively associate with the cytokine receptor and act as docking sites for signaling molecules[71]. The intensity and duration of cytokine signaling seems to be regulated by several mechanisms, involving the protein inhibitors of activated STATs (PIAS) and the suppressor of cytokine signaling (SOCS protein)[69]. SOCS genes are induced by cytokines and can inhibit cytokine signaling by binding to downstream signaling molecules. SOCS proteins are tightly regulated but are extremely labile too, and proteasome inhibitors decrease their degradation[72].

TRIM8 is a suppressor of cytokine signaling-1 (SOCS-1) interacting protein. *TRIM8* mRNA can be induced by IFNγ in murine B lymphoid M12 cells, murine fibroblasts and HeLa cells and the N-terminal 204 aminoacids of TRIM8 interact with SOCS-1. TRIM8 accelerates the degradation of SOCS-1, probably through its E3-ubiquitin ligase activity. This destabilizing action on SOCS-1 prevents SOCS-1-mediated inhibition of IFNγ, activating JAK-STAT pathway[69]. Therefore,

TRIM8 may be a regulator of SOCS-1 function in the IFNγ pro-inflammatory pathway, exerting its oncogenic role (Fig. 6)[69].

1.5.3. TRIM8 in the regulation of STAT3

1.5.3.1. The JAK/STAT pathway

Another important pathway tightly regulated by TRIM8 and important for stemness and oncogenesis, places TRIM8 in a positive feedback loop with the JAK/STAT signaling.

The JAK/STAT signaling pathway transduces information originated from cytokines extracellular signals finally regulating DNA transcription of genes important for cell proliferation, differentiation, and apoptosis[73]. STAT proteins (STATs) belong to a family of transcription factors that are activated by polypeptide ligands, such as cytokines and growth factors. STATs comprise seven members: STAT1, STAT2, STAT3, STAT4, STAT5 (a/b) and STAT6[74]. Among them, STAT3 is a crucial member of the STAT family, which forms a dimer following activation, enters the nucleus, and regulates the transcription of diverse target genes[75].

STAT3 protein contains six functional domains: i) N-terminal domain (ND), which is able to stabilize the dimerized STAT3 and promotes the formation of tetramers of two STAT3 dimers to make it more stable with DNA; ii) coiled-coil domain (CCD), which mediates STAT3 direct binding to the receptor and facilitates STAT3 phosphorylation on 705-tyrosine site (Y705); iii) DNA binding domain (DBD), which, by recognizing the specific sequences on DNA, will direct STAT3 to the promoters of target genes to initiate the transcriptional activation ; iv) the linker region, the function of which is unknown at present; v) Src homology 2 (SH2) domain, the most conserved part of STAT3, which plays a critical role in the process of signal transduction through STAT3 phosphorylation and subsequent dimerization; vi) C-terminal transcriptional activation domain (TAD), in which is located the STAT3 phosphorylation on 727-tyrosine site (Y727)[73].

The Janus kinase (JAK) family consists of four non-receptor tyrosine kinases, JAK1, JAK2, JAK3 and tyrosine kinase 2 (TYK2), which phosphorylate a number of signaling molecules that contain specific SH2 domain[76]. Different cytokine receptors on the cell membrane bind the corresponding ligands to form homologous or heterodimers, which drive the mutual phosphorylation of the JAKs in proximity, and facilitate the activation of STAT3. STAT3 phosphorylation at the Y705 and/or the Y727 site, leads to the activation and dimerization of STAT3, which will rapidly enter the nucleus, specifically bind to the STAT inducible element sequences (SIE), and initiate the activation and transcription of target genes[73].

The activity of STAT3 in the nucleus is tightly controlled by two negative regulators, SOCS and PIAS. In particular, PIAS is an important negative regulator of STAT3 activity[77]. PIAS3 affects STAT3 activation via several molecular mechanisms: i) the inhibition of transcription by blocking

the DNA-binding activity of p-STAT3; ii) the suppression of transcription by recruiting other co-regulators, including histone deacetylases; iii) the sumoylation of p-STAT3; iv) the suppression of transcription by sequestering p-STAT3 to certain sub-nuclear structures where co-repressor complexes are enriched[78].

1.5.3.2. The TRIM8-PIAS3-STAT3 loop

STAT3 has a broad range of biological functions, including cell activation, cell proliferation and apoptosis. Activated STAT3 has been shown to protect tumor cells from apoptosis and promote cell proliferation by regulating genes encoding antiapoptotic and proliferation-associated proteins[79].

In this regulation mechanism, TRIM8 controls STAT3 activation interacting with PIAS3 and i) degradating PIAS3 through the ubiquitin- proteasome pathway, ii) excluding PIAS3 from the nucleus, through the interaction with heat shock protein 90β (Hsp90β) and consequently modulating *Nanog* transcription in embryonic stem cells[80, 81].

In the first case, TRIM8 physically interacts with PIAS3, determining its monoubiquitylation and consequently contributing to the proteasomal degradation of PIAS3, destabilizing its structure. Moreover TRIM8, that is a nuclear protein, causes the disruption of the nuclear localization of PIAS3, translocating it in the cytosolic fraction and excluding PIAS3 from the nucleus[80]. Consequently, TRIM8 induces a down-regulation of the PIAS3-STAT3 interaction thus positively regulating STAT3-dependent gene expression and thereby inducing oncogenesis[80].

STAT3 plays an important role in leukemia inhibitory factor (LIF) signaling pathway in embryonic stem (ES) cells to maintain their pluripotent state. LIF-dependent signaling pathways in mouse ES cells also modulate different signals, including *Nanog* transcription[81]. In ES cells, heat shock protein 90β (Hsp90β) interacts with STAT3 and accelerates STAT3 nuclear translocation, thus regulating LIF signaling[82]. In this context TRIM8 binds Hsp90β and consequently modulates the translocation of phosphorylated STAT3 into the nucleus. Accordingly, TRIM8-knockdown results in an accumulation of a large amount of total STAT3 and tyrosine 705 (Y705)-phosphorilated STAT3 in the nucleus and in a down-regulation of *Nanog* transcription. Thus, TRIM8 modulates the interaction between STAT3 and *Nanog* promoter region through the chaperon activity of Hsp90β, suggesting that TRIM8 has an important role in the regulation of STAT3-mediated signaling in the differentiation and self renewal of ES cells[81].

1.5.3.3. TRIM8 and STAT3 regulate stemness in glioblastoma

TRIM8 also has a role in maintaining stemness and self-renewing capabilities of glioblastoma multiforme stem-like cells (GSCs) through the activation of STAT3 signaling[83] (Fig. 7).

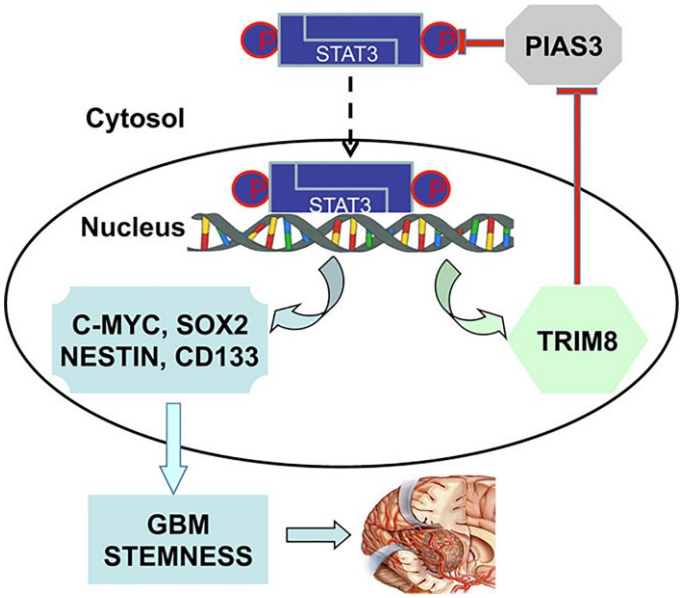

Figure 7. Schematic model of the TRIM8-PIAS3-STAT3 pathway that regulates glioblastoma stemness. TRIM8 suppresses PIAS3 through proteasomal degradation, resulting in enhanced activation of STAT3. STAT3 promotes GSC stemness factors SOX2, NESTIN, CD133, and c-MYC. In addition, STAT3 promotes TRIM8 expression, forming a positive bidirectional regulatory loop involving TRIM8 and STAT3.

TRIM8 expression in GSCs positively correlates with GSC markers NESTIN and CD133 as well as the stem cells transcription factors c-MYC and SOX2, thus maintaining the self-renewing capability of these cells. Moreover, TRIM8 expression is strongly and positively correlated with STAT3, SOX2, NESTIN, Olig2, Nanog and BMI suggesting that TRIM8 is relevant to GBM stemness[83]. Interestingly, in patient-derived GBM neurospheres, TRIM8 overexpression correlates with STAT3 upregulation and PIAS3 suppression. Conversely, after *TRIM8* knockdown, PIAS3 expression increases and reduces the expression levels of activated STAT3[83]. Since TRIM8 overexpression reduces the half-life of PIAS3 of about 2 hours, Zhang et al. demonstrated that TRIM8 suppresses PIAS3, most likely through ubiquitin-mediated proteasomal degradation, leading to upregulation and activation of STAT3[83].

Moreover, in GSCs there is a strong positive mRNA correlation between TRIM8 and STAT3. Interestingly, *TRIM8* promoter region contains two transcription factor binding sites (TFBS) for STAT3, and TRIM8 shows a parallel dose-dependent increase in protein expression, in response to IL-6, known to potently induce STAT3 activation in GSC and regulate their self-renewal capacity[84, 85]. Therefore, STAT3 activation contributes to TRIM8 expression in GBM neurosphere cells and TRIM8 regulates GBM neurosphere stemness through a bidirectional positive feedback loop involving PIAS3 and STAT3[83] (Fig. 7).

2. AIM OF THE THESIS

Since E3 ubiquitin ligase proteins regulate carcinogenesis through the timely control of many cellular processes such as DNA damage response, metabolism, transcription, and apoptosis[76, 86-88], we reasoned that the TRIM8 activity might impact on cell transcriptome patterns, thereby promoting cancer development and progression. Moreover, to gain further insights into TRIM8 function in brain biology, we searched for putative novel TRIM8 protein partners using a proteomic approach combined with Mass Spectrometry.

The identification of TRIM8-related transcript and substrate signatures was carried out on normal embryonic neural stem cells (eNSC) infected with a retrovirus expressing FLAG-Trim8 or an empty vector. NSCs display molecular hallmarks of forebrain radial glia and can be considered as the "bona fide" healthy counterpart of glioma cells[89]. Moreover, in vitro culture of neural stem cells has proven to be a valuable experimental approach for exploring molecular processes in disease models of the central nervous system (CNS)[90]. Firstly, we profiled the whole transcriptome of normal eNSC infected with a retrovirus expressing FLAG-Trim8 by using RNA-Seq, to assess the differential gene expression perturbations due to TRIM8 overexpression and to identify several genes and transcripts. Then, a proteomic approach based on TRIM8 immunoprecipitation (IP) assays coupled to LC-MS/MS in eNSC, allowed us to detect a plethora of TRIM8 interacting proteins (Fig. 8). Both transcriptomic and proteomic data were analyzed with several bioinformatics tools to define protein networks and pathways relevant for gliomagenesis.

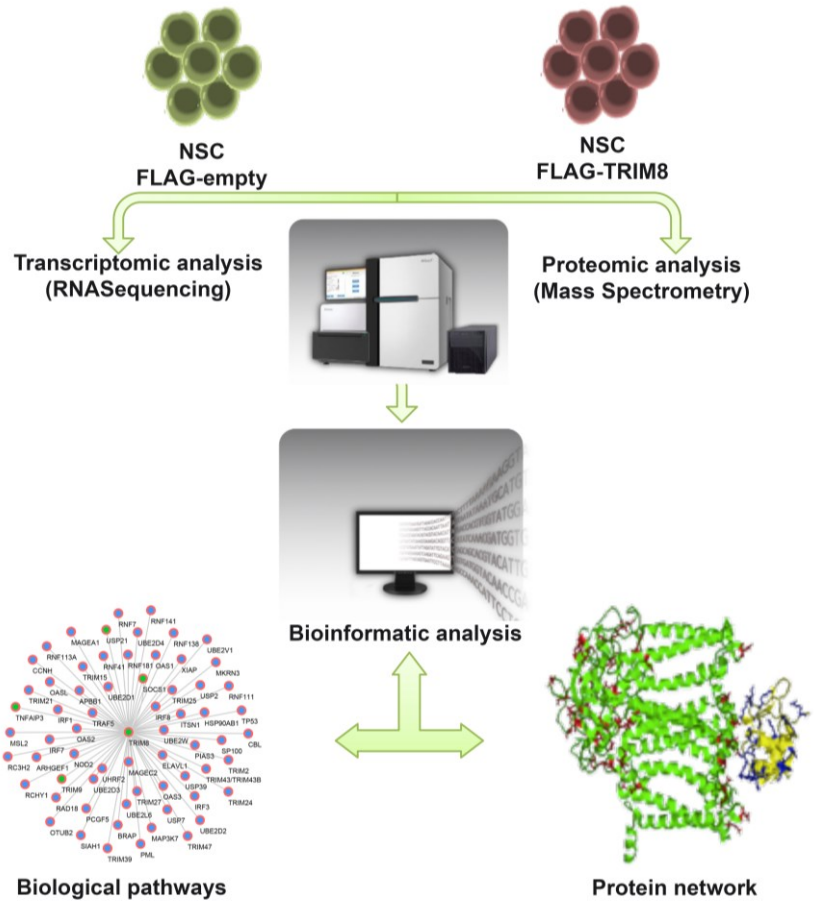

Figure 8. Experimental strategy. Embryonic neural stem cells (eNSC) are infected with a retrovirus expressing FLAG-Trim8 or an empty vector. We obtained TRIM8-related biological pathways and protein network through both RNA-Seq and Mass Spectrometry analysis, examined with bioinformatics tools.

Overall this thesis aims to i) profile *TRIM8*-related transcriptome to identify TRIM8 particular substrates and glioma-related biological pathways; ii) profiling TRIM8-related interactome to classify TRIM8 protein network and specific interactors highly relevant for gliomagenesis; iii) exploring the effect of TRIM8 and TRIM8-targeted substrates and interactors on biological networks relevant for cancer progression.

The possibility of selectively targeting TRIM8 expression or TRIM8 substrates and/or interactors will provide a unique opportunity to translate the generated knowledge into the clinical setting in the form of TRIM8-based therapeutics.

3. MATERIAL AND METHODS

3.1. Cell lines

Murine embryonic neurospheres were established starting from E14 telencephalic progenitors obtained as described in[91]. Briefly, E14 telencephalic emispheres were dissected from the brain and dissociated in 1 ml of Trypsin/EDTA (Life Technologies) for 15 minutes at 37 °C. DMEM medium with 10% fetal bovine serum (Thermo Fisher Scientific) was then added and cells were mechanically dissociated with a Pasteur pipette. After centrifugation for 5 minutes at 500 RCF, cells were resuspended in neural stem cells medium (DMEM/F12 from Thermo Fisher Scientific, 1× B27 supplement from Thermo Fisher Scientific, 10 ng/ml EGF from Peprotech, 10 ng/ml bFGF from Peprotech) and seeded in 24 well plates (50,000–150,000 cells/well). After plating, cells were infected with replication in competent retrovirus expressing the murine FLAG-tagged Trim8 sequence and a GFP cassette or a control vector expressing only the GFP cassette. After a short period of expansion in vitro, infected cells were FACS-sorted to obtain a pure population of GFP-positive cells that were used for RNA-Seq analysis. Human fibroblasts were maintained in DMEMF12 while HEK293, Hela and U87MG cell lines were maintained in DMEM with Glutamax medium. Both medium were supplemented with 10% fetal bovine serum and 1% antibiotics (Thermo Fisher Scientific).

3.2. Retroviral vectors

The murine FLAG-tagged Trim8 sequence was cloned in the pCAG:GFP MMLV retroviral vector (kindly provided by Dr. M. Goetz, Institute of Stem Cell Research, Germany), upstream the IRES–GFP reporter cassette. As control vector we used the same pCAG:GFP vector expressing only the IRES-GFP cassette. Replication-defective retroviral supernatants were prepared by transiently transfecting plasmids into Phoenix packaging cells and harvesting the supernatant after 2 days. The supernatants were concentrated by centrifugation and stored at −80 °C before use.

3.3. RNA-Seq library preparation and sequencing

Total RNA was extracted using mini RNase kit reagent (Qiagen) and treated with DNase-RNase free (Qiagen). RNA integrity was evaluated by using the Agilent 2100 Bioanalyzer (Agilent Technologies). Next generation sequencing experiments were performed by Genomix4Life S.r.l. (Baronissi, Italy). Indexed libraries were prepared from purified RNA with the TruSeq Total Stranded RNA Sample Prep Kit (Illumina) according to the manufacturer's instructions. Libraries were quantified using the Agilent 2100 Bioanalyzer (Agilent Technologies). Indextagged samples were equimolar and the overall concentration was 2 nM. The pooled samples were subject to cluster generation and sequenced using an Illumina HiSeq 2500 System (Illumina) in a 2×100 paired-end format at a final concentration of 8 pmol.

3.4. Pre-processing and mapping reads to the mouse reference genome

RNA-Seq yielded an average number of 68,5 million reads per sample, ranging from 60 to 86 million reads. Raw data (.fastq files) were quality-controlled using the FastQC v0.11.5 software package and exhibited an average quality score as high as 36 (phred). Reads were discarded if the average per-base phred values were<20 or trimmed by Trimmomatic[92] if the phred values of>5% of nucleotides at the extremities of the reads were lower than 20. Residual adapter sequences were removed by cutadapt.>75% of the paired-end reads were mapped to the GRCm38 mouse reference genome by TopHat 2. To summarize the alignments statistics, the resulting BAM files were analysed using SAMtools.

3.5. Differential expression and survival analyses

Uniquely mapped reads were counted and RPKM-normalized. To assess the cross-sample consistency of the expression profiles, the Pearson's correlation coefficient was calculated for each pairwise combination of samples. Differential gene expression was obtained by one-way ANOVA, as implemented in Partek® Genomics Suite® version 6.6, if Benjamini-Hochberg's FDR-adjusted p-values<.05. Any random batch effect was mitigated by the Batch Effect Removal® tool of Partek. Differentially expressed genes were subjected to Gene Set Enrichment Analysis (GSEA) by Ingenuity® Pathway Analysis (IPA®, Qiagen, Summer 2017 Release). The whole procedure of functional enrichment analysis was based on the prior calculation of the activation z-scores, by which we inferred the activation states of biological functions and pathways. An enrichment score (Fisher's exact test, p-value), instead, was calculated to measure the overlap between observed and predicted deregulated gene sets. We considered p-values <.05, with positive or negative z-scores indicating predicted activated or inhibited functions/pathways. Categories of functional annotations were ranked by a score computed with the weighted sum of the absolute z-scores of the diseases and functions belonging to the categories. Weights were calculated as the complement of the inverse of -log p-value (pv), as reported in[93]. Correlation of expression between functionally relevant genes and TRIM8 was checked in The Cancer Genome Atlas (TCGA; https:// cancergenome.nih.gov/) cohort of glioma tissues (530 Low Grade Gliomas and 166 Glioblastomas) through Spearman correlation test. Considering the high variability of the gene expression profiles of these tumor samples, a minimum correlation value of 0.2 was set. The Log-Rank test was used to compare the survival distributions of two samples divided according to the mean expression values of TRIM8 and of other relevant genes. Samples having expression levels greater than the mean value were assigned to the High group, while samples with the expression values less or equal to the mean were assigned to the Low group. All statistical computations were made through R statistical software (R version 3.3.2).

3.6. PCR arrays validation of RNA-Seq differential expressed genes

Mouse embryonic neurospheres were infected with a retrovirus expressing FLAG-Trim8 or with an empty vector. Total RNA was extracted using mini RNase kit reagent (Qiagen), treated with DNase-RNase free (Qiagen), quantified by Nanodrop (Thermo Fisher Scientific) and reverse-transcribed using RT2 First Strand Kit (Qiagen) according to the manufacturer's instructions. Resulting complementary DNA from each sample was aliquoted both into mouse Jak-Stat signalling RT2 Profiler™ PCR arrays (Qiagen/SABiosciences catalog no. PAMM-039Y, gene list provided online). Real-time PCRs were performed on an ABI 7900 (Thermo Fisher Scientific-Applied Biosystems). Data were analysed by using RT2 Profiler PCR Array data analysis software (www. SABiosciencies.com/pcrarraydataanalysis.php), provided by SABiosciences.

3.7. Quantitative real time PCR

Total RNA from mouse embryonic neurospheres infected with a retrovirus expressing FLAG-Trim8 or with an empty vector was reverse transcribed using the Quantitect Transcription kit (Qiagen), according to the manufacturer's instructions. Oligos for qPCR were designed using the Primer express program[94] with default parameters. *GAPDH* and *ACTIN* were used as reference genes. The reactions were run in triplicate in 10 ul of final volume with 10 ng of sample cDNA, 0.3mM of each primer, and 1XPower SYBR Green PCR Master Mix (Thermo Fisher Scientific-Applied Biosystems). Reactions were set up in a 384-well plate format with a Biomeck 2000 (Beckmann Coulter) and run in an ABI Prism7900HT (Thermo Fisher Scientific-Applied Biosystems) with default amplification conditions. Raw Ct values were obtained using SDS 2.3 (Applied Biosystems). Calculations were carried out by the comparative Ct method as reported in[95]. Significance was determined by a two-tailed unpaired t-test for means.

3.8. Dual-luciferase assay

HEK293 and U87MG cells were plated in 12-wells culture dishes at a density of 4×10^4 cells/ml and then co-transfected with a pNanoLuc- SIE reporter vector (Promega), pGL3-basic FireFly (Promega) and pDEST-EGFP-STAT3, p3xFLAG-TRIM8 or p3xFLAG-TRIM8 b-box deletion mutant constructs, using Lipofectamine® LTX (Thermo Fisher Scientific) according to the manufacturer's instructions. 48 h after transfection, firefly luciferase activity was monitored using the Dual-GLO® Luciferase Assay System (Promega) in a Glomax 96 microplate luminometer and was normalized to the Nano luciferase activity of the pNanoLuc-SIE vector for each transfected well.

3.9. Co-immunoprecipitation and western blot

HEK293 and U87MG cells were plated in 100mm culture dishes at a density of 5×10^5 cells/ml, transfected with the indicated plasmids. After 48 h, cells were lysed in RIPA buffer. Total lysates

cells were co-immunoprecipitated with anti-FLAG (Sigma) or anti-EGFP (Santa Cruz) using Dynabeads magnetic beads (Thermo Fisher Scientific) following manufacturer's instructions. Complexes were analyzed by SDS page electrophoresis and blotted with the indicated antibodies. Horseradish peroxidase conjugated anti-mouse (Santa Cruz) and anti-rabbit (Santa Cruz) antibodies and the ECL chemiluminescence system (GE Healthcare) was used for detection.

3.10. Isolation of nuclear and cytoplasmic extract

HEK293 and U87MG cells were plated in 60mm culture dishes transfected with the indicated plasmids. After 48 h, cells were harvested and fractionated. Nuclear and cytoplasmic extraction was prepared using an NE-PER Nuclear Cytoplasmic Extraction Reagent kit (Pierce) according to the manufacturer's instruction. Protein concentrations of cytoplasmic and nuclear extracts were measured using the Pierce 660 nm protein assay (Thermo Fisher Scientific) with the GloMax Discover System (Promega). Nuclear and cytoplasmic extracts were resolved by SDS page electrophoresis and blotted with anti-STAT3 (79D7, Cell Signaling), anti-Phospho-STAT3 (Tyr705, Cell Signaling), anti-LaminB (Santa Cruz) and anti-αtubulin (Sigma). ImageJ software was used to quantify band signal intensity. Values are expressed as fold differences relative to the endogenous STAT3 protein, set at 1.

3.11. DNA-binding assay

HEK293 cells were plated in 100mm culture dishes at a density of 5×10^5 cells/ml, transfected with the indicated plasmids. After 48 hours, cells were lysed in RIPA buffer. Protein concentrations of cell lysates were measured as described above and incubated with the immobilized STAT3 Consensus Oligonucleotide Sepharose conjugate (Stat3 Consensus oligonucleotide sequence: 5'-GATCCTTCTGGGAATTCCTAGATC-3′) (Santa Cruz, sc-2571 AC) in binding buffer, according to the manufacturer's instruction. Samples were centrifuged, washed and eluted from the beads by using Elution Buffer. Then, SDS–PAGE was performed.

3.12. Cell sonication

HEK293 and U87MG cells were plated in 60mm culture dishes and transfected with FLAG-TRIM8, EGFP-STAT3 and/or empty vectors. 48 hours after transfection, cell pellets were lysed in RIPA buffer and then the suspension was sonicated with a microtip attached to UP50H sonifier, 40% amplitude, and constant power 12 times for 60 s, allowing the suspension to cool on ice for 1 minute between pulses. After sonication, the spread of size fragments was checked by running 1 µl of total cell lysate on a 1% agarose gel.

3.13. Immunoprecipitation and mass spectrometry analysis.

Mouse embryonic neurospheres were lysate in Lysis Buffer (150mM NaCl, 50mM Tris-HCl, pH 7.4, 1mM PMSF, 1% NP-40, and cocktail of proteases inhibitors). Total protein extracts were pre-

cleared and incubated overnight at 4°C with M2 anti-FLAG magnetic-conjugated antibodies beads (Sigma). Beads were washed with lysis buffer containing up to 300mM NaCl. The retained protein complexes were eluted by competition with FLAG peptide for 5 hours at 4°C. Protein components were then fractionated by 8-15% gel for SDS-PAGE and protein bands, stained with colloidal blue Coomassie (Pierce), were excised from the gel and subjected to proteomic procedure for protein identification[96]. Nanoscale liquid chromatography coupled to tandem mass spectrometry (nanoLC-MS/MS) analyses of peptide mixtures were performed on a LTQ-Orbitrap mass spectrometer (ThermoFisher Scientific) equipped with a nano-electrospray ion source and coupled with a nanoEasy-LC II capillary HPLC system (Proxeon Biosystem). Samples were injected onto a capillary chromatographic system consisting of a 2 cm length trapping column (C18, ID 100um, 5um) and a 10 cm C18 reverse phase silica capillary column (ID 75um, 3um) (ThermoFisher Scientific). A gradient of 80 minutes of acetonitrile eluents was used for separation (0.3 μ L/min flow rate). Mass spectrometry analysis was performed with a resolution set to 30,000 and a mass range from m/z 200 to 1800 Da. The five most intense doubly and triply charged ions were selected and fragmented in the ion trap. All MS/MS samples were analyzed using licensed Mascot software (Matrix Science) to search the UniProt database for *mus musculus* taxonomy. Searches were performed with 1-missed cleavage allowed, carbamidomethylcysteine as fixed modification, pyro-GLU with N-terminal glutamine, pyro-carbamidomethylcysteine with N-terminal CAM-CYS, methionine oxidation as variable modifications.

3.14.Silencing experiments.

Stealth RNAi duplexes against human *TRIM8* (Thermo Fisher Scientific, TRIM8HSS129955; TRIM8HSS129956; TRIM8HSS188606) and stealth RNAi negative control (Thermo Fisher Scientific) were transfected in HeLa, HF and U87MG cells using Lipofectamine RNAiMAX (Thermo Fisher Scientific) according to the manufacturer's protocol. TRIM8-silencing was confirmed by Western Blot analysis using anti-TRIM8 C-20 (Santa Cruz) and by qPCR.

3.15.Fluorescence and confocal microscopy.

Immunostaining analysis were carried out as reported in[95]. Cells were seeded on glass coverslips and, 24 hours after RNA interference, fixed with 100% methanol, incubated in blocking solution containing PBS and 1% bovine serum albumin (BSA), and counterstained with α-TRIM8 (1:500, Sigma), α-tubulin antibody (1:1000, Sigma), γ-tubulin antibody (1:1000, Sigma). After an incubation with Alexa Fluor 568 goat anti-rabbit IgG, Alexa Fluor 568 goat anti-mouse IgG, Alexa Fluor 488 goat anti-rabbit IgG, Alexa Fluor 488 goat anti-mouse IgG (1:500, Thermo Fisher Scientific) followed by DAPI (Molecular Probes), immunostained cells were covered with a drop of mounting medium, observed and examined with a Zeiss Axiovert microscope equipped with LSM-

780-META module and Leica TCS SP8 confocal microscopy (Leica, Wetzlar, Germany). Images were captured, pseudo-colored and analyzed by Leica LAS AF software.

3.16. Live-cell imaging.

Cells were seeded on 8-well slides (80826, ibiTreat, Ibidi) and observed under an inverted microscope (Eclipse Ti - Nikon) using a 40x objective. During the observation, cells were kept in a microscope stage incubator at 37°C and 5% CO_2. Images were acquired over a 24 hours period by using a DS-Qi1Mc camera. Image and video processing were performed with NIS-Elements AR 3.22.

3.17. Cell synchronization.

Cell synchronization was carried out on HeLa cells by plating cells onto 12 multi-well plates; after Stealth RNAi transfection (as described in silencing experiments section) Cells were treated with 4 mM thymidine in complete medium for 12 hours, washed twice with PBS, incubated for 12 hours in complete medium, and treated again for 12 hours with 4 mM thymidine in complete medium. The resulting G1/S-enriched cells were washed twice with PBS and released into the cell cycle in the presence of DMEM-10% FBS until the harvest time.

3.18. Metaphase Spreads and Karyotyping.

Human primary fibroblasts transiently transfected with control or *TRIM8* shRNAs were treated with 50ng/mL Colcemid (Invitrogen-Life Technologies) for 2 hours before proceeding with metaphases preparations. Cells were collected and resuspended in a hypotonic solution of 2% KCl and 2% $Na_3C_6H_5O_7$ for 7 minutes at 37°C. Metaphase spreads were then prepared and stained with Giemsa-trypsin (G-band) procedure. Analysis was carried out using the OLYMPUS BX41 microscope equipped with a BASLER scA1400-17gmASI digital camera. Images were analyzed using the Applied Spectral Imaging (ASI) software V7.0.6.8860. Unless stated differently, for each experiment at least one hundred metaphases for each sample were counted.

3.19. Flow cytometric analysis

HeLa synchronized cells were collected over indicated time points and fixed in 100% ethanol for 30 minutes at -20°C. Fixed cells were treated with RNaseA (Sigma) for 20 minutes at room temperature. Cell cycle was determined by DNA stained with propidum iodide (Sigma) 10µg/ml in PBS. Flow cytometries were performed by MoFlo® Astrios^{TM} (Beckman Coulter) and the data analyzed by FlowJo software (TreeStar).

4. RESULTS

4.1. TRIM8-driven transcriptomic profile identified glioma-related nodal genes and pathways

4.1.1. TRIM8-related transcriptomic profile

RNA-Seq revealed 1365 differentially expressed transcripts of 912 genes (Fig. 9A). 723 of them (corresponding to 648 RefSeq genes) differed significantly of at least 1.5 folds (192 upregulated transcripts of 178 genes and 531 downregulated transcripts of 470 genes). We next performed a pathway enrichment analysis obtaining that 80 genes, among all differentially expressed genes, significantly enrich 18 pathways by IPA analysis (Fig. 9B; table is not shown). 53% of these genes (43 out of 80 genes) are related to cell-morphology, cell death and survival, with a preponderantly representation of signalling pathways related to neurotransmission and to CNS, including axonal guidance, GABA Receptor, ephrin B, synaptic long-term potentiation/depression, and glutamate receptor (Fig. 9B; Tab. 1). Focusing on signaling pathways related to neurotransmission and to the CNS, we found that four out of five CNS-related pathways have in common the *M-RAS* gene (NM_008624, p-value=.0060, FC=−1.54), which encodes for a member of the Ras family of the small GTPases, specifically expressed in brain and heart (Fig. 9C, Tab. 1). Moreover, two out of five CNS-related pathways, the glutamate receptor and synaptic long-term potentiation/depression signalling, share *GRM8* (NM_008174, p-value=.010, FC=−2.24), *GRM1* (NM_001114333, pvalue=. 036, FC=8.19), and *GRIA4* (NM_0011, p-value=.044, FC=1.68) genes (Fig. 9C).

4.1.2. Gene set functional enrichment analysis

In a research of the most represented over-represented diseases and biological functions, we performed a gene set enrichment analysis that yielded 68 significantly represented biological functions grouped into different processes (Fig. 9D, table is not shown). These line up with the classes of enriched pathways, which can be ascribed in neurological, neurotransmission, transport and cellular organization-related functions. Among the differentially expressed genes, *VEGF* (NM_001110268, p-value=.017, FC=−16) is the most pleiotropic gene, since it participates to 51 out of 68 biological functions (Tab. 1) and 4 pathways out of 18 (table is not shown).

Ingenuity Canonical Pathways	-log(p-value)	z-score	Molecules
Leukocyte Extravasation Signaling	2.95E00	-1.897	CLDN10,CLDN19,MMP14,ITGB3,TEC,NCF1,CLDN12, RAP1GAP,SIPA1,PECAM1,RASSF5,CTNNB1,OPN1SW ,ITK
Axonal Guidance Signaling	2.37E00	NaN	GNG4,ADAM22,RGS3,NRP2,BMP8A,MYLPF,SEMA6B, VEGF,MYL6B,SLIT2,NFATC1,LIMK1,VEGFA,EFNA5,E FNB1,MRAS,ADAM23,RASSF5,WNT5B,OPN1SW,ACE ,SEMA7A
Calcium Signaling	2E00	-0.447	CAMK2D,TNNT3,Tpm1,TNNI3,RYR1,MYL6B,CHRNA10 ,GRIA4,RCAN2,SLC8B1,NFATC1
Ephrin B Signaling	1.83E00	-1.000	GNG4,RGS3,EFNB1,MRAS,CTNNB1,LIMK1

Synaptic Long Term Potentiation	1.79E00	-0.378	CAMK2D,GRM8,GRM1,PPP1R1A,PPP1R3C,**MRAS**,CACNA1C,GRIA4
Endoplasmic Reticulum Stress Pathway	1.73E00	NaN	HSP90B1,MAP3K5,HSPA5
Glutamate Receptor Signaling	1.71E00	NaN	GRM8,GRM1,SLC1A2,HOMER3,GRIA4
Ephrin Receptor Signaling	1.67E00	-1.000	VEGFA,GNG4,RGS3,SORBS1,EFNA5,EFNB1,**MRAS**,**VEGF**,FGF1,LIMK1
Insulin Receptor Signaling	1.55E00	-1.134	SCNN1A,TSC1,SGK1,PPP1R3C,ASIC3,**MRAS**,LIPE,SLC2A4
Cardiac β-adrenergic Signaling	1.53E00	-1.134	GNG4,PPP1R1A,PPP1R3C,PDE1B,**MRAS**,CACNA1C,PDE11A,PPP2R1B
Bladder Cancer Signaling	1.5E00	NaN	VEGFA,FGF18,MMP14,**MRAS**,**VEGF**,FGF1
GABA Receptor Signaling	1.44E00	-1.000	KCNN4,GABRA4,GABRB1,**MRAS**,ALDH9A1
Synaptic Long Term Depression	1.39E00	-0.707	PLA2G16,GRM8,GRM1,**MRAS**,RYR1,PPP2R1B,GRIA4,Gucy1b2
eNOS Signaling	1.39E00	-1.890	VEGFA,HSP90B1,LPAR1,**VEGF**,CHRNA10,CASP8,HSPA5,Gucy1b2
Gα12/13 Signaling	1.38E00	-2.646	TEC,LPAR1,MYLPF,**MRAS**,MYL6B,MAP3K5,CTNNB1
Pyrimidine Ribonucleotides Interconversion	1.36E00	NaN	ENTPD1,ENTPD6,AK7
Oleate Biosynthesis II (Animals)	1.32E00	NaN	UFSP1,FADS2
Gustation Pathway	1.32E00	NaN	SCNN1A,ASIC3,PDE1B,P2RX1,P2RX5,PDE11A,P2RX2

Table 1. List of over-represented canonical pathways (enrichment p-value, activation z-score and list of molecules).

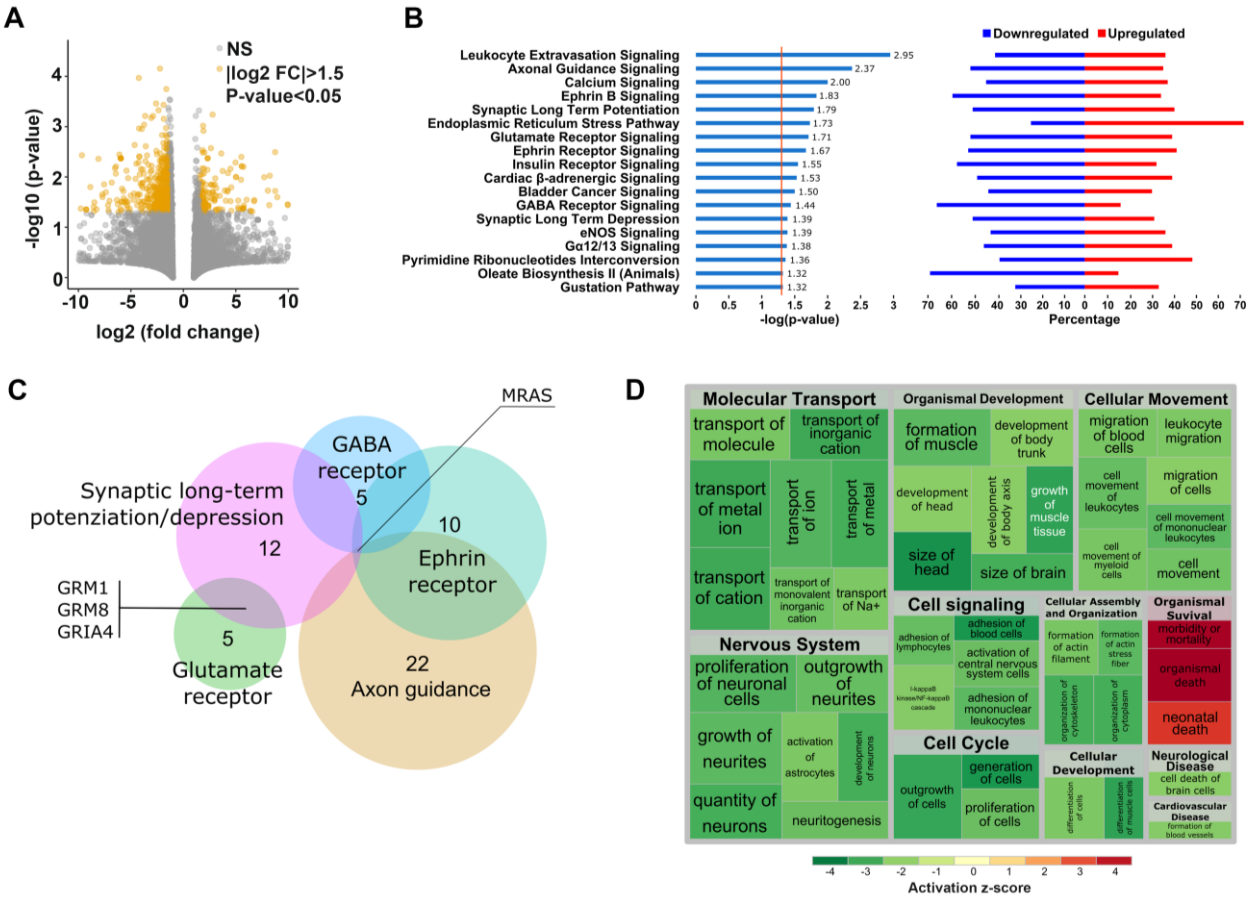

Figure 9. TRIM8-related transcriptomic profile in neural stem cells. (A) Volcano plot of 722 differentially expressed transcripts (orange-coloured). **(B)** Forest plot (left) reporting 18 significantly enriched pathways, log(p-value) > 1.3; Stacked bar plot (right) accounting for proportions of upregulated and downregulated genes for each pathway. **(C)** EULER diagram representing the number of genes participating to five signalling pathways related to neurotransmission and to the CNS. **(D)** Treemap representing over-represented diseases and biological functions, grouped into processes, as calculated by IPA. Predicted activated processes are coloured in red, while inhibited processes are coloured in green, according to the inferred zs. Sizes of squares are proportional to -log(p-values). The greater a square, the more significant the enrichment of the function it corresponds to.

4.1.3. Validation of RNA-Seq data

RNA-Seq analysis revealed a set of genes that resulted differentially expressed. In order to validate this result, we measured the expression of *GRIA4*, *GRM1*, *GRM8*, *MRAS*, and *VEGFA* genes by qPCR analysis on eNSC infected with a retrovirus expressing FLAG-Trim8, compared to that of control cells. Accordingly with the RNA-Seq data, we showed an up-regulation of *GRIA4* and *GRM1* (FC: 2.37; 2.26, respectively) and a down-regulation of *GRM8*, *MRAS*, and *VEGFA* (FC: 0.5; 0.86; 0.37, respectively) (Fig. 10A).

Interestingly, the pathways enrichment analysis revealed a perturbation of many genes related to the JAK-STAT signaling pathway. Therefore, we verified the differential expression of a set of genes associated to JAK/STAT using a commercial PCR array. The panel of mouse genes includes nuclear co-factors, receptors and co-activators associated with the Stat proteins, Stat-inducible genes, and negative regulators of the Jak-Stat pathway. We monitored a global dysregulation of the Jak-Stat pathway in accordance to RNA-Seq data in eNSC infected with a retrovirus expressing FLAG-Trim8, compared to control cells (Fig. 10B). For instance, *Epor*, *Jak1*, and *Smad5* were found significantly down-regulated while *Stat3* up-regulated in overexpressing FLAG-Trim8 eNSC, compared to control cells, respectively.

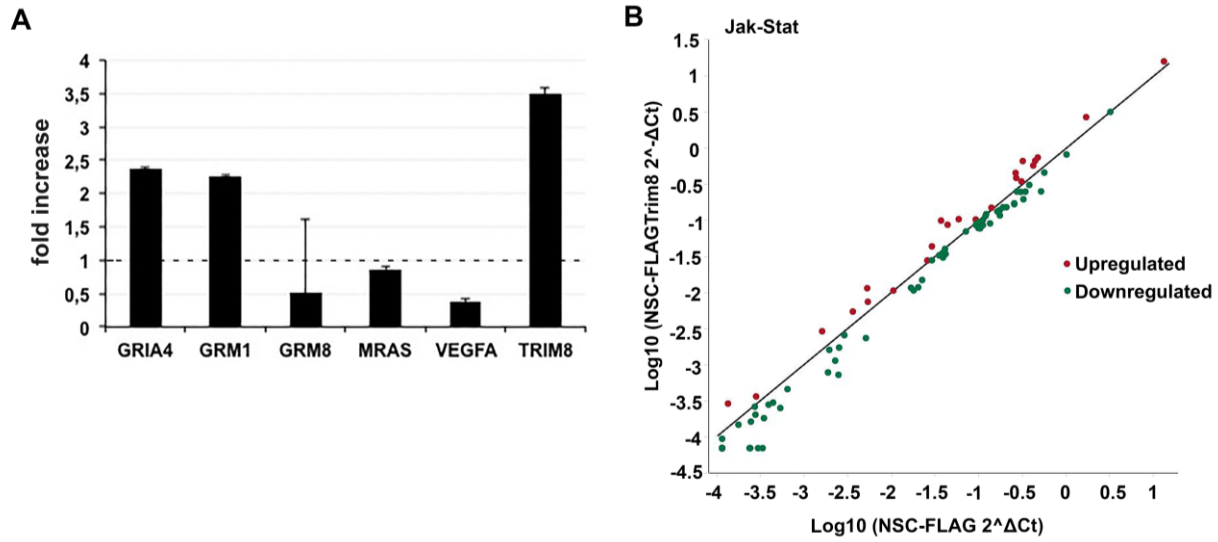

Figure 10. Validation of RNASeq data. (A) qPCR analyses were carried out on eNSC infected with a retrovirus expressing FLAG-TRIM8 or FLAG as control. Data were normalized to the expression of β-actin and L41. Bar represents the average of three replicated experiments±standard errors. **(B)** The graph plots the log10 of normalized expression levels of every gene on the array in a control condition (eNSC-expressing only tag, x-axis) versus an experimental condition (eNSC-expressing FLAG-tagged Trim8, y-axis). Scatter plot: Jak-Stat PCR array, PAMM-

039Y. The central line indicates unchanged gene expression. Symbols outside the delimited area indicate fold-differences larger than a threshold that we set to 1. The red symbol in the upper-left corner readily identifies up-regulated genes, and the green symbols in the lower right corner readily identify down-regulated genes. Values were derived by taking the means of fold changes of three biological replicates per time point.

4.1.4. Correlation of CNS and glioma-related genes expression with TRIM8 in TCGA cohort

Recently, we evidenced a significant increase in the risk of death and disease progression in WHO grade III gliomas with low TRIM8 expression levels compared to those with high mRNA levels[(53)]. Our expression data showed that the transcriptional levels of a number of CNS- and glioma-related genes, such as *GRIA4*, *GRM1*, *GRM8*, *EPOR*, *SMAD5*, *MRAS*, *STAT3*, and *VEGFA*, were significantly perturbed by TRIM8 expression. Therefore, we investigated whether a correlation may exist between the transcriptional level of *TRIM8* and these brain-related genes in a cohort of 530 Low Grade Glioma (LGG) and 166 Glioblastoma (GB) tissues from The Cancer Genome Atlas (TCGA) Research Network. The analysis revealed a significant positive correlation in LGG cohort between the expression of *TRIM8* and *GRIA4*, while a significant negative correlation was found between *TRIM8* and *STAT3* and *VEGFA*. With regard to the GB cohort, *TRIM8* expression positively correlates with *GRM1* and *STAT3* transcriptional levels (Fig. 11A).

In order to examine the prognostic value of combined *TRIM8* expression with the transcriptional levels of the above selected genes, we performed a survival analysis through Log-Rank test in the TCGA cohort of LGG and GB tissues. Survival analysis estimated a significant decrease of death-risk in LGG patients with: i) high *TRIM8* expression associates to low *GRIA4* expression, compared with low *TRIM8* and low *GRIA4*; ii) high *TRIM8* with high *VEGFA* or *STAT3*, compared with low *TRIM8* and high *VEGFA* or *STAT3*. Analyzing GB tissues, Kaplan-Meier survival curves highlighted that high *TRIM8* expression with low *STAT3*, compared with high *TRIM8* and high *STAT3*, was co-related to favorable clinical outcomes in glioma patients (Fig. 11B). These data suggested that such expression combination might be a useful supplement to the repertoire of clinicians for predicting survival time of glioma patients and that the ability to use just one or a handful of genes to predict outcome could have an impact on therapeutic treatments.

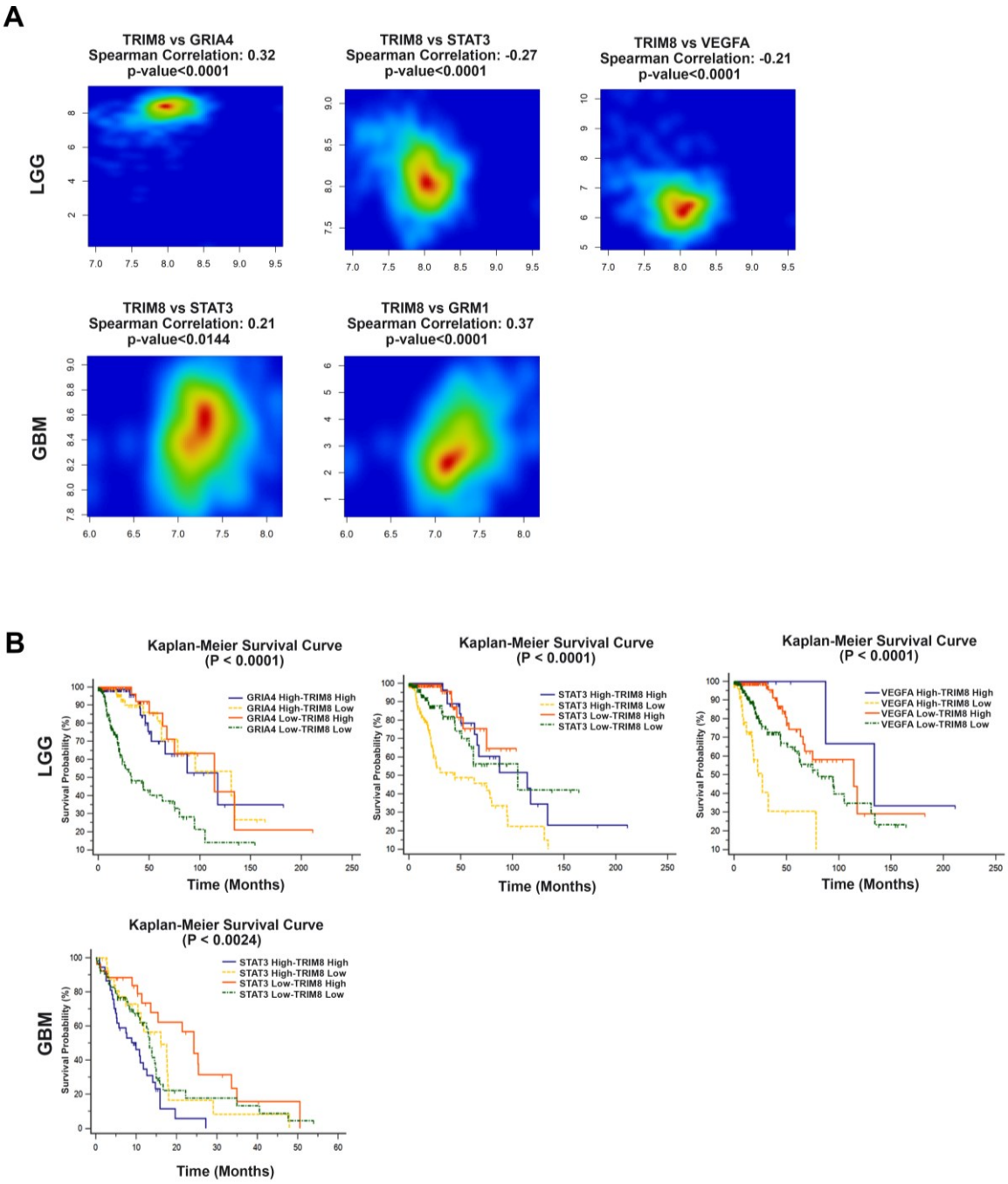

Figure 11. Correlation of CNS and glioma-related genes expression with TRIM8 in TCGA cohort. (A) Spearman correlation between *TRIM8* and *GRIA4*, *STAT3*, *VEGFA*, and *GRM1* transcriptional levels. Graphical representation of log-transformed RPKM of 6 genes identified by RNA-Seq in a cohort of LGG and GB of The Cancer Genome Atlas Research Network (y axis) and *TRIM8* (x axis). Colors represent the density of observations at paired expression values. Higher densities are represented by red regions and lower densities are in blue, while yellow and green regions have intermediate densities that go from higher to lower, respectively. **(B)** Kaplan-Meier curves for Overall Survival according to RNA-Seq FPKM from LGG and GB TCGA data. We performed the Log-Rank test between the combinations of *TRIM8* expression groups and those made by other relevant genes.

4.1.5. TRIM8 physically interacts with STAT3

Our results showed that both *STAT3* and *TRIM8* expressions were significantly correlated in glioma tissues and associated to clinical outcomes in glioma patients. Therefore, based on all these evidences, we investigated the TRIM8-STAT3 loop.

Co-immunoprecipitation experiments demonstrated that overexpressed TRIM8 and STAT3 self-associate in both HEK293 (Fig. 12A-B) and U87MG cells (Fig. 12C). To delineate the minimal motif regions involved in TRIM8-STAT3 interaction, we used a set of STAT3 and TRIM8 deletion mutants (Fig. 12D). We found that TRIM8 interacts with all STAT3 mutants, but with the C-terminal construct expressing only the transactivation domain, from amino acid 688 to the end of the STAT3 protein. This data suggests that the SH2 domain of STAT3 is required for the efficient binding of TRIM8. The physical interaction between TRIM8 and STAT3 persisted also when we used STAT3Y705F, a construct expressing a dominant-negative STAT3 mutant harboring a substitution of tyrosine 705 to phenylalanine, which fails to be phosphorylated, suggesting that the STAT3 phosphorylation status is dispensable for TRIM8 interaction (Fig. 12E). Finally, to understand if even some TRIM8 specific domains were involved in this interaction, we tested the TRIM8 deletion mutants, founding that all mutants retain the ability to interact with STAT3 (Fig. 12D-F).

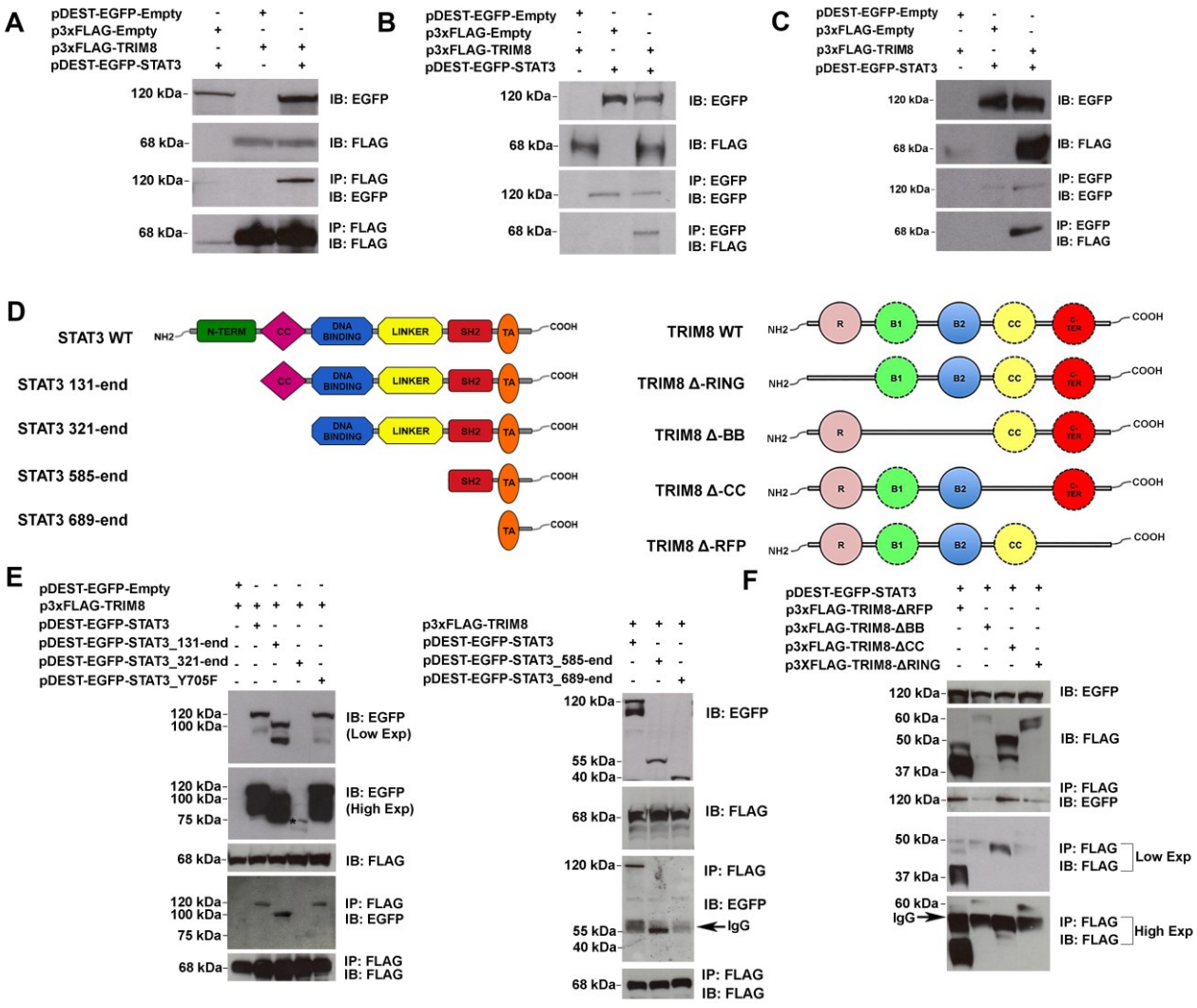

Figure 12. TRIM8 and STAT3 self-associate through STAT3 SH2 domain. (A-B) Whole protein lysates of HEK293 and U87MG **(C)** cells transfected with the indicated plasmids, were separated on 10% SDS-PAGE gel and

subjected to immunoblotting with anti-EGFP and anti-FLAG. **(D)** Schematic representation of STAT3 and TRIM8 structural domains and deletion mutants (SH2: Src Homology 2; TA: transactivation; R: ring; B1-B2: BBox 1–2; CC: coiled coil; Cterm: C terminal). **(E)** HEK293 cells were transfected with indicated STAT3 wild type and mutants together with or without FLAG-tagged TRIM8, immunoprecipitated with anti-FLAG and followed by immunoblot as shown. (* indicates the specific band at an higher exposition time). **(F)** HEK293 cells were transfected with indicated plasmids encoding TRIM8 mutants together with or without EGFP-tagged STAT3. The immunoprecipitated complexes were analysed by immunoblotting with anti-EGFP and anti-FLAG (low and high exposure).

Several evidences show that TRIM8 has a nuclear localization signal and that acts as a shuttle to favor the compartmentalization of many cellular proteins[6,81]. Starting with this, we next demonstrated that TRIM8 is able to bind STAT3 in the cytoplasmic cellular compartment as revealed by co-immunoprecipitation assays performed on HEK293 (Fig. 13A) and U87MG nuclear and cytoplasmic fractions (Fig. 13B).

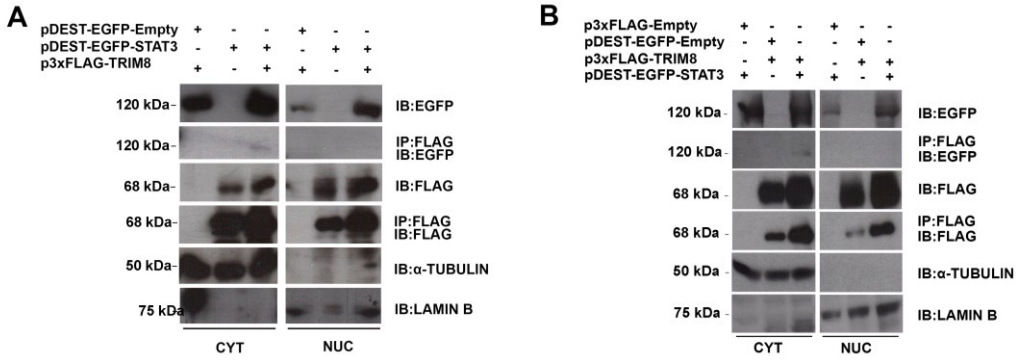

Figure 13. TRIM8 binds STAT3 in the cytoplasmic fraction. (A-B) Whole protein lysates of HEK293 (A) and U87MG (B) cells transfected with indicated plasmids were processed to obtain nuclear and cytoplasmic fractions, then co-immunoprecipitated with anti-FLAG; the immunocomplexes were separated on 10% SDS-PAGE gel and subjected to immunoblotting with EGFP, FLAG antibodies; Lamin B and α-tubulin antibodies were used to control nuclear and cytoplasmic fractions, respectively.

4.1.6. TRIM8 promotes STAT3 transcriptional activity

As STAT3 activity is finely regulated to ensure proper functions, TRIM8-STAT3 interaction raised the possibility that TRIM8 might modulate STAT3 transcriptional potential. To explore this, we monitored TRIM8 effect on STAT3 transcriptional activation. We performed luciferase reporter assays in HEK293 and U87MG cells using a Nano Luc vector containing the STAT3-inducible element (SIE) (NanoLuc-SIE) upstream of the luciferase reporter gene (Fig. 14). In this assay, the stronger the STAT3 transcriptional activity is, the more binding there will be with the SIE and we will consequently detect a greater reporter gene signal.

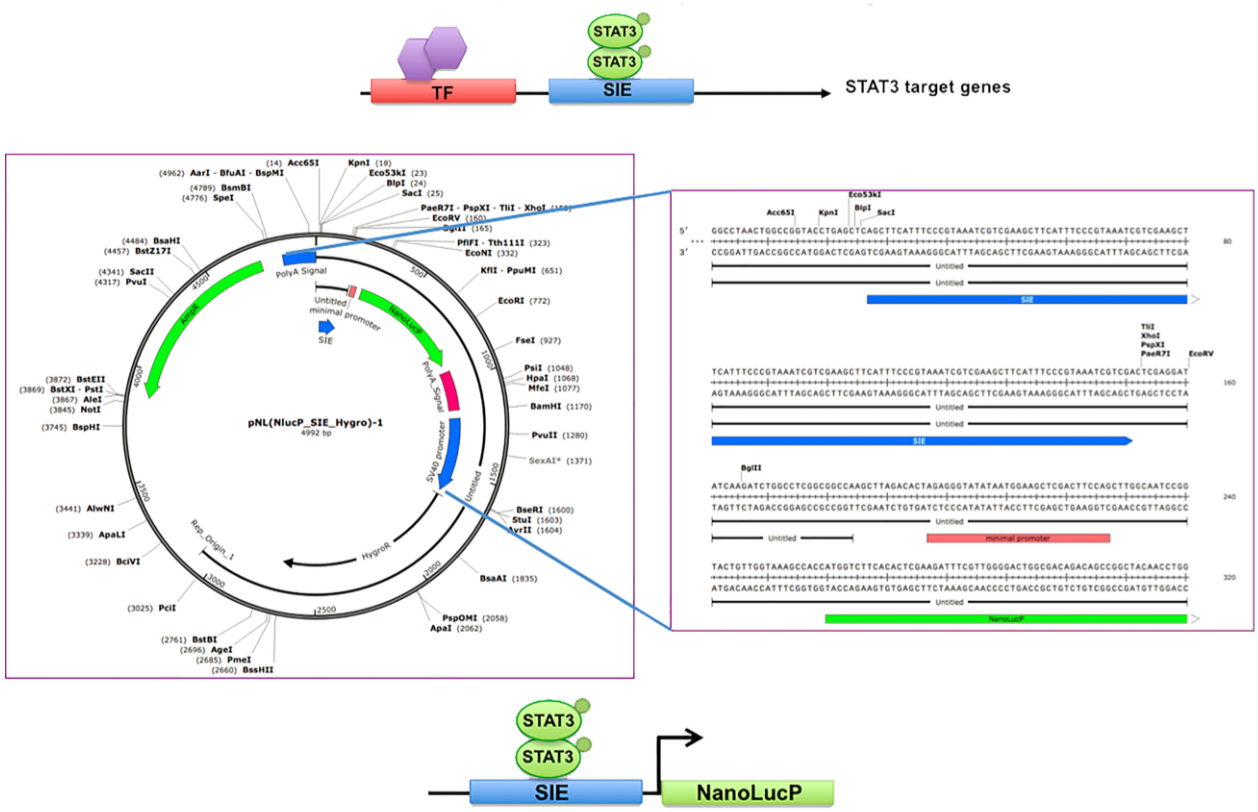

Figure 14. Schematic representation of the NanoLuc-SIE expression vector. The pNL vector (NlucP_SIE_Hygro)-1 consists of a reporter gene (green) downstream of the STAT3 inducible elements (SIE) (blue). The STAT3 binding to the SIE sequences regulates the activation and subsequent transcription of the reporter gene which encodes for the luciferase.

We found a 1.7 and 1.8 significant fold increase of luciferase signal in HEK293 cells expressing exogenous STAT3 or TRIM8, respectively. Interestingly, we detected a 2.7 fold increase of the reporter activation in cells co-expressing STAT3 and TRIM8 (Fig. 15A). Accordingly, we observed a 5.7 fold increase of reporter activation in U87MG cells co-expressing STAT3 and TRIM8 (Fig. 15B). Interestingly, the inhibition of TRIM8 expression by using specific siRNAs reduced the luciferase reporter activity induced by STAT3 (Fig. 15C). Overall these data suggested that TRIM8 plays a role in the SIE-mediated luciferase transactivation and that its function might be mediated by endogenous STAT3. These evidences allowed us to hypothesize that TRIM8 might work together with STAT3 to potentiate the reporter activation. Next, we investigated the effects of TRIM8 domains in SIE binding and reporter activation by performing luciferase assays with a set of FLAG-tagged TRIM8 deletion mutants (Fig. 15D). We detected that all TRIM8 mutants partially decreased the luciferase activation both alone and when co-expressed with STAT3, suggesting the importance of TRIM8 integrity in the STAT3 activity regulation (Fig. 12D). This activity is not mediated by the nuclear STAT3Y705 phosphorylation status, which is generally believed to be essential for STAT3's transcriptional activity[97], as no changes were observed in STAT3Y705 protein levels (Fig. 15 E-F).

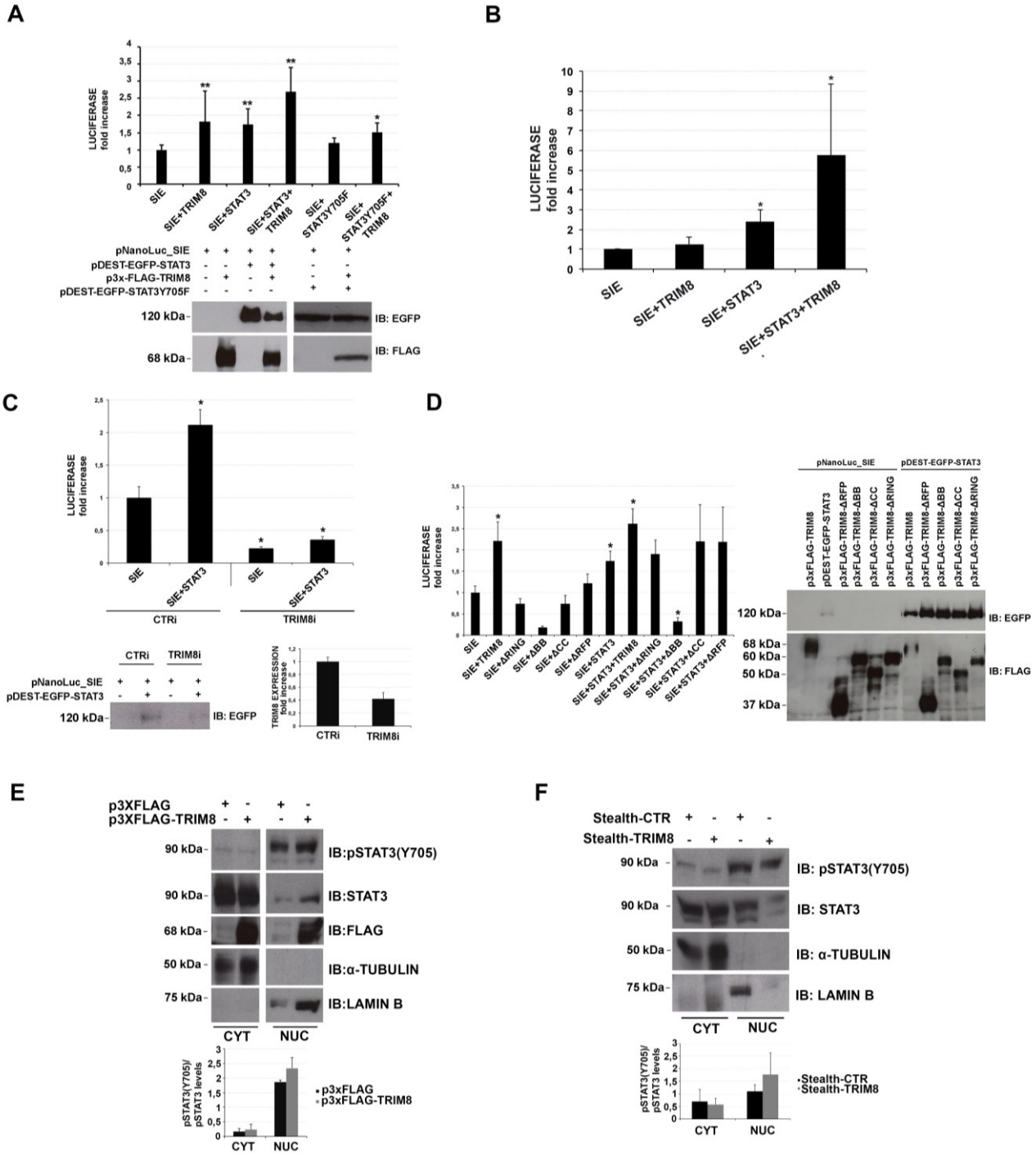

Figure 15. TRIM8 interacts with STAT3 to promote STAT3 transcriptional activity (A) Luciferase assays were performed in HEK293 and **(B)** U87MG cells co-transfected with a pNanoLuc-SIE reporter vector, pGL3-basic FireFly and pDEST-EGFP-STAT3, p3xFLAG-TRIM8 as indicated. **(C)** Luciferase assays were carried out in HEK293 cells transfected with control and TRIM8 stealths and then co-transfected with a pNanoLuc-SIE reporter vector, pGL3-basic FireFly, pDEST-EGFPSTAT3 or pDEST-EGFP-STAT3Y705F, as shown. **(D)** Luciferase assays were performed in HEK293 cells co-transfected with a pNanoLuc-SIE reporter vector, pGL3- basic FireFly and indicated plasmids. Luciferase activities were normalized to the level of FireFly luciferase. Each bar represents the average of three independent experiments±standard error (**: p<.01; *: p<.05); total lysates from HEK293 cells used for luciferase assays in A, B and D were separated on 10% SDS-PAGE gel and subjected to western blot analysis using the indicated antibodies. **(E)** Whole protein lysates of U87MG cells transfected with indicated plasmids, were processed to obtain nuclear and cytoplasmic fractions, then separated on 10% SDS-PAGE gel and subjected to immunoblotting with EGFP, FLAG, pSTAT3(Y705), STAT3, α-tubulin and LaminB1 antibodies. **(F)** U87MG transfected with Stealth RNAi (Stealth-control; Stealth-TRIM8) were lysed and processed to obtain nuclear and cytoplasmic fractions. Extracts were

separated on 10% SDS-PAGE gel subjected to immunoblotting with the indicated antibodies. (D, E) up: Lamin B1 and α-tubulin antibodies were used to control nuclear and cytoplasmic fractions, respectively. (CYT: cytoplasmic fraction; NUC: nuclear fraction); down: quantification of pSTAT3(Y705) normalized on total STAT3. The intensity of pSTAT3 and STAT3 bands were quantified using ImageJ software. Each bar represents the average of two independent experiments ± standard error.

4.1.7. TRIM8 directly binds SIE-sequences

Starting from the observation that TRIM8 enhances STAT3 transcriptional activity and that has an independent activity on STAT3 target genes, we next investigated whether the TRIM8 function on STAT3 transactivation is mediated by the TRIM8 binding to SIE. For this purpose, we monitored the TRIM8 presence at STAT3 consensus sequence in cellular extracts obtained from HEK293 cells overexpressing FLAG-TRIM8 treated with and immobilized to STAT3 Consensus Oligonucleotide (Santa Cruz)-Sepharose conjugate, a particular co-precipitation technique that allows to identify proteins that are stably bound to the STAT3-binding nucleotide sequence[(98)]. The precipitates were subjected to western blot analysis. We detected TRIM8 bound to the STAT3 DNA-consensus in all the cellular precipitates except for that of negative control (Fig. 16A). These data supported that TRIM8 binds the STAT3 DNA-consensus. To assess whether SIE DNA regions participate to TRIM8-STAT3 interaction, we performed co-immunoprecipitation experiments after removing DNA from HEK293 total lysates. We found the STAT3-TRIM8 interaction still persisted also in the absence of the DNA, suggesting that SIE regions are not essential for the physical interaction (Fig. 16 B-C). All together our data demonstrated a functional loop between TRIM8 and STAT3 in both HEK293 and U87MG glioma cell lines.

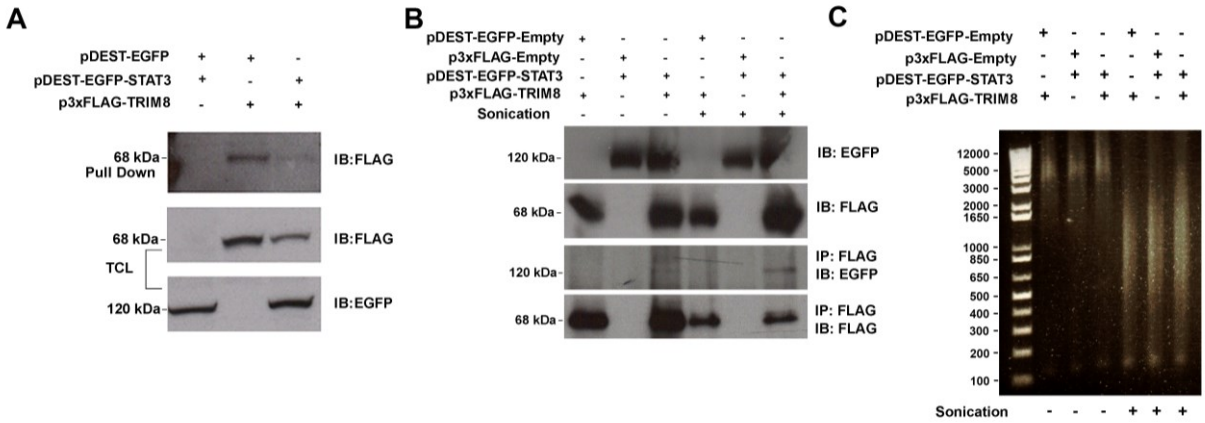

Figure 16. TRIM8 directly binds SIE-sequences. (A) HEK293 cells were transfected with pDEST-EGFP-STAT3, p3xFLAG-TRIM8 or empty vector and after 48 h were stimulated with IL-6 (20 ng/ml) for 30 min. To measure STAT3 and TRIM8 DNA binding, cell extracts were treated with the immobilized STAT3 Consensus Oligonucleotide (Santa Cruz)-Sepharose conjugates. The precipitates were subjected to western blot analysis with FLAG and EGFP antibodies. An aliquot of total cell lysate (TCL) was blotted with the same antibodies. **(B)** HEK293 cells were transfected with the indicated plasmids and harvested after 48 h. Cell lysed suspensions in lanes 4–6 were sonicated with a microtip attached to UP50H sonifier 12 times for 60 s, amplitude 40%, cycle 1. Cell lysates were then co-immunoprecipitated with anti-FLAG; the immunocomplexes were separated on 10% SDS-PAGE gel and subjected to immunoblotting with EGFP and FLAG antibodies. **(C)** Electrophoretic analyses of genomic DNA of HEK293 cells not subjected to sonication (lanes 1-3) and subjected to sonication 12 times for 60 seconds, amplitude 40%, (lanes 4-6).

4.2. TRIM8-driven proteomic profile identifies its role in the mitotic spindle machinery

4.2.1. TRIM8 physically interacts with mitotic proteins

To gain further insights into TRIM8 function in brain biology, we searched for putative novel TRIM8 protein partners using a proteomic approach combined with mass spectrometry in primary mouse embryonic neural stem (eNSC) cells. We infected eNSC cells with a retrovirus expressing FLAG-tagged Trim8 or an empty vector and we performed anti-FLAG pull-down experiments from total protein lysates. FLAG-containing immunoprecipitated complexes were fractionated by SDS-PAGE and then analyzed by LC-MS/MS. Fifty TRIM8 putative interacting proteins were identified and subsequently categorized on the basis of UniProt annotations for functional processes and pathways, including proteins involved in transcription, signal transduction/protein modification, and protein traffic/microtubule based movement (Fig. 17A). Interestingly, the main represented group of TRIM8 potential interactors (22%) consisted of protein involved in the mitotic spindle assembly (Tab. 2). Hence, we first validated a subset of the identified mitosis-associated proteins with a different score of peptide numbers. Total cell lysates of HEK293 cells co-transfected with vectors expressing Flag-tagged Trim8 or EGFP empty vector and EGFP-tagged KIF11, Kif2c, KIFC1, or Haus1, were Flag pulled-down and subjected to Western blot analysis. We found that Trim8 co-immunoprecipitates with KIF11, Kif2c, KIFC1, and Haus1 (Fig. 17B), strongly confirming the proteomic data.

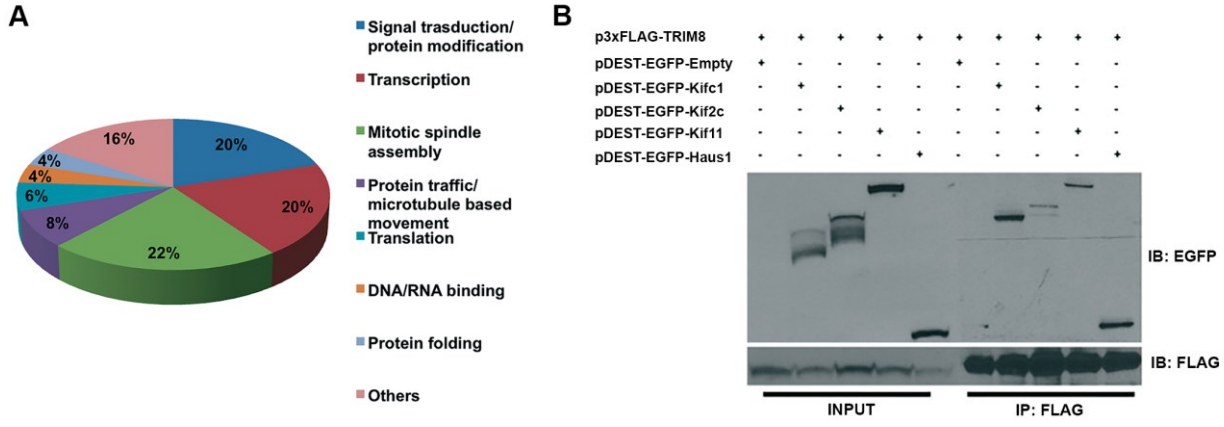

Figure 17. TRIM8 is involved in the mitotic process. (A) Functional classification of TRIM8 interacting proteins. **(B)** HEK293 overexpressing FLAG-TRIM8 and EGFP-KIFC1, -KIF2C, -KIF11 or -HAUS1 were lysed and immunoprecipitated with anti-FLAG and blotted with indicated antibodies

Protein Name	Gene name	Number of Peptides	MW(kDa)	UniProt Code
Condensin complex sub. 2	Ncaph	12	83	Q8C156
Kinesin-like protein KIF11	Kif11	11	119	Q6P9P6
MTSS1-like protein	Mtss1l	10	77	Q6P9S0
Protein bicaudal D homolog	Bicd2	6	94	Q921C5
Kinesin-like protein KIF20B	Kif20b	5	205	Q80WE4

Centrosomal protein of 170 kDa	Cep170	5	176	Q6A065
La-related protein 4	Larp4	5	80	Q8BWW4
Kinesin-like protein KIF2C	Kif2c	4	82	Q922S8
HAUS augmin-like complex subunit 1	Haus1	4	31	Q8BHX1
Kinesin-like protein KIFC1	Kifc1	3	75	Q9QWT9
Four and a half LIM domains protein 3	Fhl3	2	34	Q9R059

Table 2: Putative TRIM8 interacting proteins involved in the mitotic spindle assembly The list of putative Trim8 protein partners associated with the mitotic spindle assembly according with UniProt functional annotation and literature information and identified by functional proteomics approach is reported. For each protein the gene name, the number of identified peptides, the molecular weight and the UniProt code are also indicated.

4.2.2. Disentangling the role of TRIM8 in the mitotic spindle processes

We next explored the role of TRIM8 in the mitotic spindle machinery functions. First, we analyzed endogenous TRIM8 cellular localization throughout the different phases of the cell cycle in HeLa cells by indirect immunofluorescence. TRIM8 predominantly localizes in nuclear aggregates in interphase cells, as previously reported[(95)]. A diffuse cytoplasmic and nuclear staining and several discrete foci were observed in prophase. During metaphase and until the anaphase transition, TRIM8 associates with the mitotic spindle and re-appears into the nucleus reforming small aggregates and concentrating at the spindle midzone and midbodies, in telophase (Fig. 18A). Consistently, TRIM8 co-localize with PLK1, a polo-like kinase protein involved in the regulation of spindle assembly and chromosome segregation, which gathers in the midbody at the end of mitosis (Fig. 18B). Finally we detected endogenous TRIM8 at centrosomes as showed by co-localization with γ- tubulin (Fig. 18C). These findings strongly suggest that TRIM8 specifically associates with important structures of the mitotic spindle machinery, during mitotic progression.

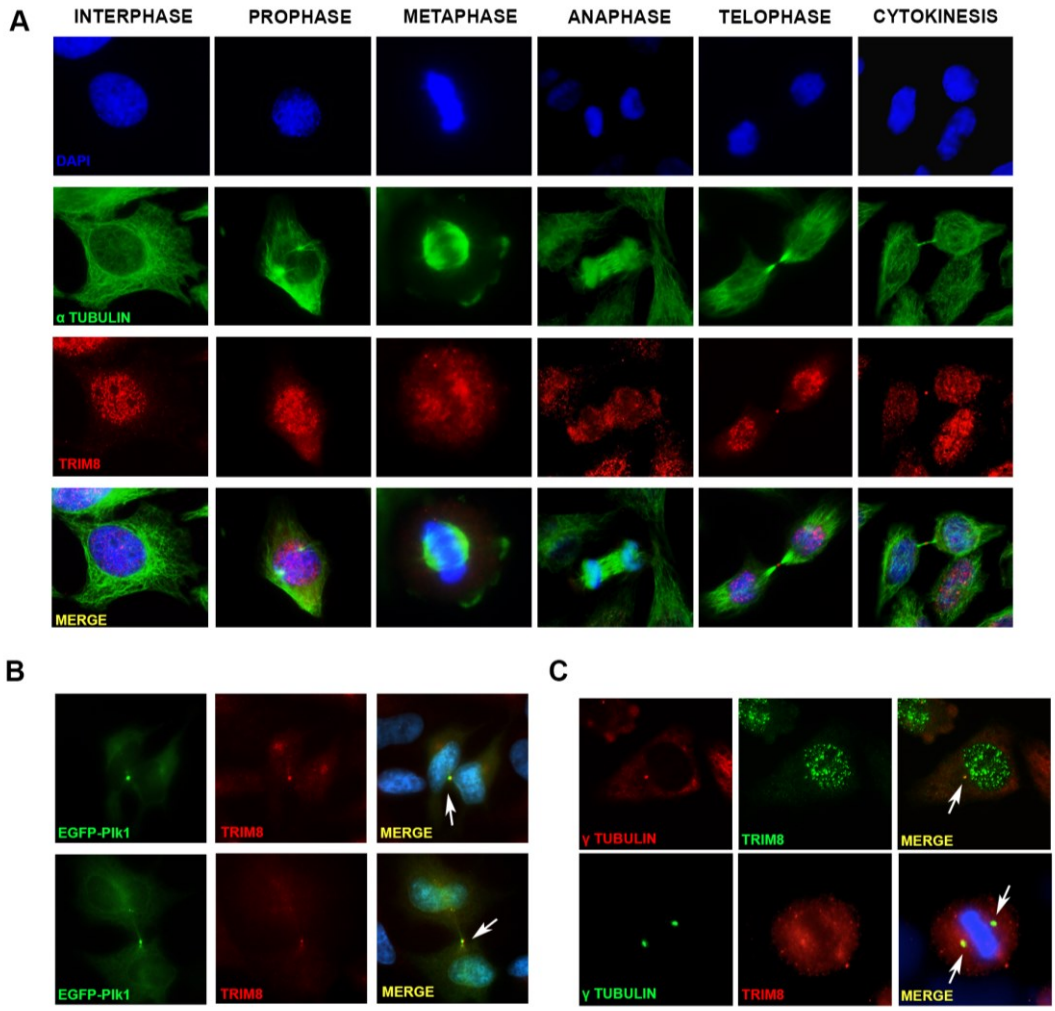

Figure 18. Localization of endogenous TRIM8 during cell cycle. (A) Immunofluorescenze microscopy in HeLa cells. HeLa cells were immunostained with anti-TRIM8 (red) and α-tubulin (green). The nucleus was stained by DAPI (blue). **(B)** The presence of TRIM8 at midbodies of HeLa cells was detected by immunostaining with anti-TRIM8 (red) and anti- EGFP to mark Plk1(green). **(C)** TRIM8 presence at centrosome of HeLa cells was detected by immunostaining with anti-TRIM8 (green, up – red, down) and γ-tubulin (red, up – green, down). The nucleus was stained by DAPI (blue). Arrows indicate TRIM8 co-localization with EGFP-Plk1 (B) and γ-tubulin (C).

4.2.3. TRIM8 silencing induces monopolar spindle cells and slows down mitosis progression

We therefore explored whether TRIM8 has any effect on the mitotic spindle organization by performing immunofluorescence assays in HeLa cells silenced for TRIM8 expression (TRIM8i) using specific Stealth RNAi and the relative control (CTR) (Fig. 19). TRIM8 silencing induced a monopolar spindle organization in 12.7 ± 1.5% analyzed metaphase cells (n=200), compared to the CTR (3.6 ± 0.5%, p= .003). Similar phenotypes were also observed in TRIM8-silenced HFs and U87MG glioma cells, 34.5±3.5% vs 17.5± 0.7% and 30.7±2.3% vs 9±2% respectively, when compared to their relative controls (Fig. 20A-B-C). Interestingly, in U87MG glioma cells, the monopolar phenotype is more evident (Fig. 20C). These data show that TRIM8 silencing results in accumulation of a monopolar phenotype, independently on the cell type.

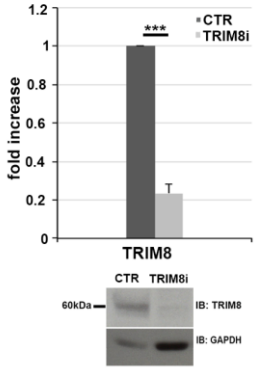

Figure 19. TRIM8 silencing by shRNA. The silencing of TRIM8 by shRNA was confirmed by immunoblot (up) and qPCR (down). Here we report a representative immunoblot on HeLa cells with anti-TRIM8 antibody; qPCR results were normalized to the expression of *EEF1A1* and *GAPDH*. Bar represents the average of three independent experiments and scale bars represent standard errors. (***p < .01).

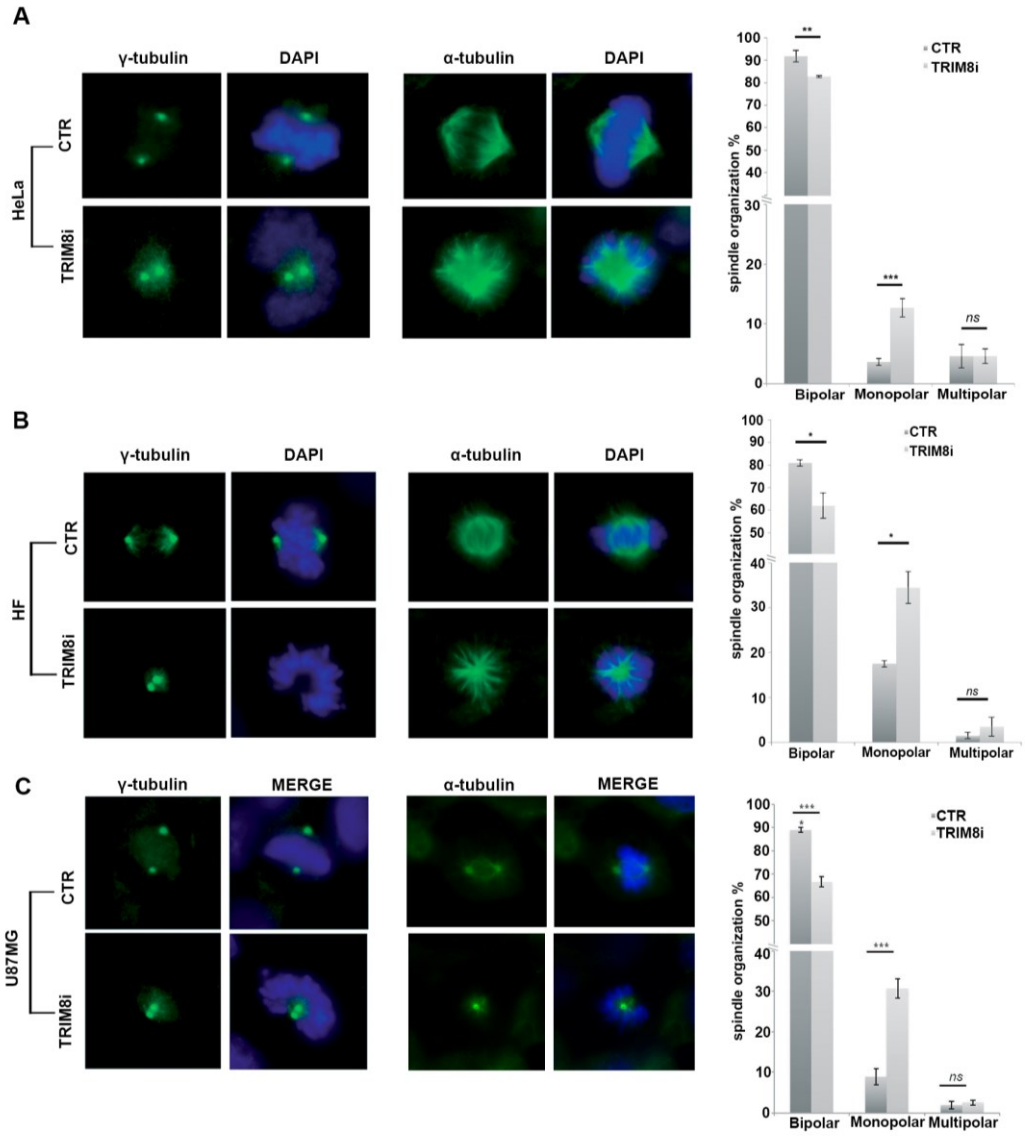

Figure 20. TRIM8 silencing induces monopolar spindles formation (A-B-C) Immunofluorescence assays were performed on HeLa, HF, and U87MG cells transfected with Stealth-TRIM8 (TRIM8i) and Stealth-control (CTR)

followed by fixing and staining with α-tubulin, (green) or γ-tubulin (green). Nuclei were visualized using DAPI. (A-B-C, left). Cells count resulted in an accumulation of monopolar spindles in HeLa, HF and U87MG. Bar represents the average of three independent experiments and scale bars represent standard errors. *p<.05; ***p<.01 (A-B-C, right).

Further, to better characterize the cytokinetic defect(s), we performed a time-lapse live-cell imaging analysis in TRIM8i- and CTR-HeLa cells. We analyzed the cytokinetic time from round up to cleavage furrow ingression. Control cells rounded up, progressed through mitosis, and started telophase within 38 min (n=114). By contrast, TRIM8-depleted HeLa cells rounded up, but remained in this phase for about 48 min (n=123) before cleavage furrow ingresses. Only 4.4% of the CTR cells started telophase after 72 min while 17.8 % of the TRIM8-silenced cells required about 113 min to complete anaphase and progress through cytokinesis (Fig. 21A-B). Together, these results show that TRIM8 participates to the formation of monopolar spindles and slows down mitosis progression, strongly supporting a role of TRIM8 in mitosis regulation.

We assessed the effect of TRIM8 during the mitosis in synchronized HeLa cells, by evaluating the protein level of Cyclin B1, a marker of mitotic entry and prometaphase to metaphase progression. After release from the second thymidine block, we found that Cyclin B1 degradation was delayed by at least one hour, in TRIM8i cells compared to CTR cells. Specifically, Cyclin B1 expression persists at 11 hours in TRIM8i cells, while in control cells Cyclin B1 expression decreased at 10 hours after the release (Fig. 21C).

To estimate the percentage of mitotic cells in TRIM8i-synchronized cells compared to control cells, we performed a flow cytometry analysis of DNA content after 8, 10, and 12 hours from the release of thymidine. We found that after 10 hours most of the cells were in G2/M phases compared to the control (33.3 vs. 26.6%). This analysis confirmed that silencing of TRIM8 induces a delay of the mitosis progression with a cell accumulation in G2/M. (Fig. 21D).

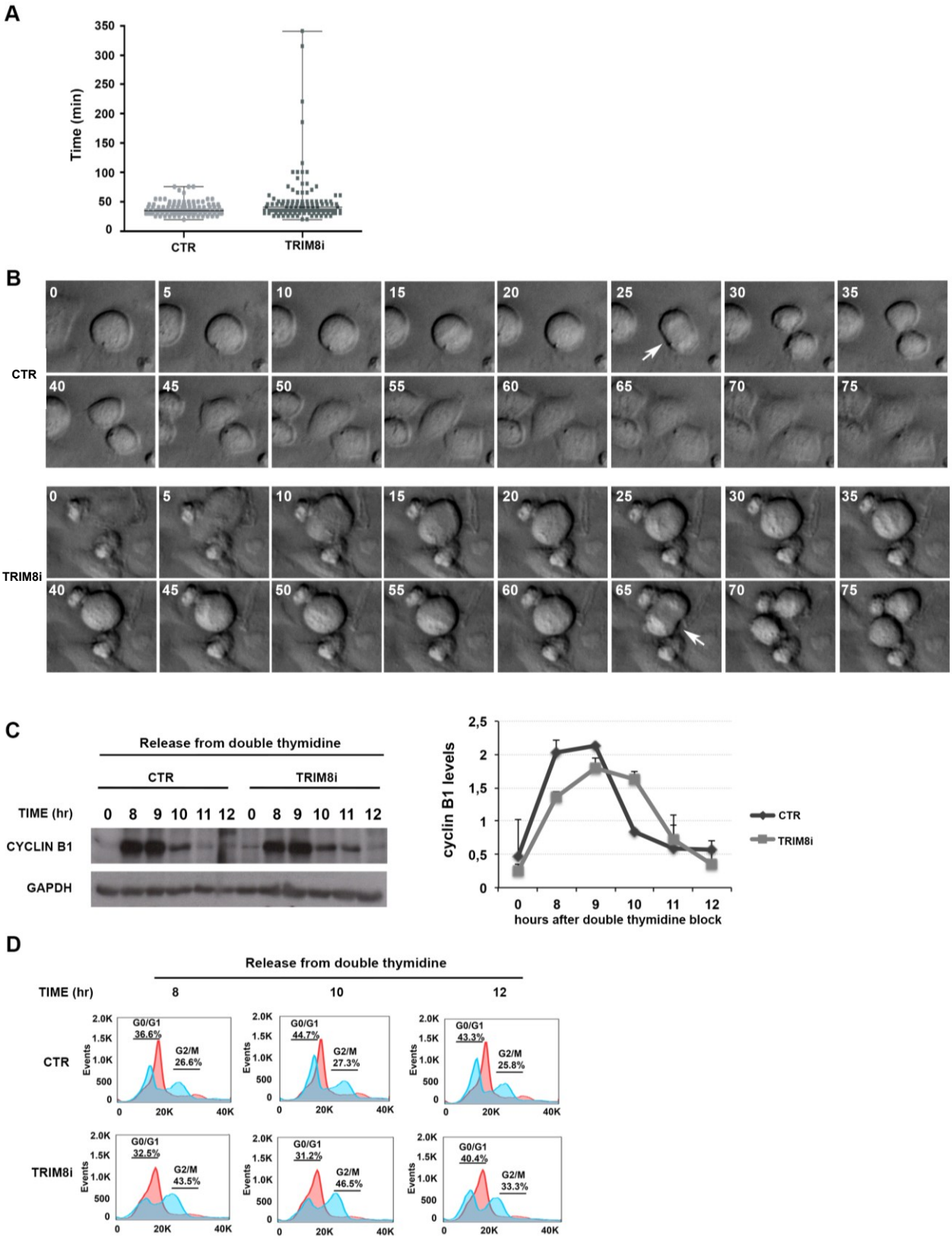

Figure 21. TRIM8 silencing induces mitosis slowdown. (A) Time lapse graph with different time points (minutes) between control and TRIM8-silenced cells (CTR;TRIM8i) to complete mitosis from the round up to the cleavage furrow ingression points. **(B)** Living HeLa controls (up) and TRIM8-silenced (down) cells were observed every five minutes. The time-lapse images obtained are shown from left to right, with time 0 indicating the round up phase. Arrows indicate the time of cleavage furrow ingression at the end of mitosis in both control (up) and TRIM8i (down) HeLa cells. Numbers indicate the times of observation. **(C)** Control and TRIM8 silenced HeLa cells were arrested by double thymidine block after TRIM8-shRNA transfection. Cyclin B1 expression was examined by western blot analysis 8-12 hours after the release from the block. GAPDH was used as loading control (left). Graph show averages calculated

on two different experiments (right). **(D)** Percentage of HeLa cells in G1, S and G2/M phases in synchronized cell cultures. HeLa control (CTR) and Hela TRIM8-silenced (TRIM8i) were harvested at indicated time points and analyzed using FACS at 10 and 12 hours after the release from double-thymidine block.

4.2.4. TRIM8 is required for chromosomal stability

As defects originating in mitosis can result in aneuploidy, we assessed the chromosomal stability in cells silenced for *TRIM8*. Counting the number of chromosomes on the metaphase spread in TRIM8i human fibroblast cells using a trypsin-Giemsa banding technique (Fig. 22A), we observed an increase of cells with less than 46 chromosomes (37% vs 16%; p=0.04) (Fig. 22B). These data were corroborated by immunofluorescence analysis that showed a significant increase of micronuclei structures in TRIM8i HFs compared to the control cells (2.9 ± 0.14% vs 1.2 ± 0.08%; p=0,0001) (Fig. 22C-D). Micronuclei represent small nucleus originating from chromosomal fragments or whole chromosomes that are not properly attached to spindle microtubules[(99)], as consequence of chromosomal instability and/or mitotic abnormalities. These data suggested that TRIM8 is important for maintaining chromosomal stability.

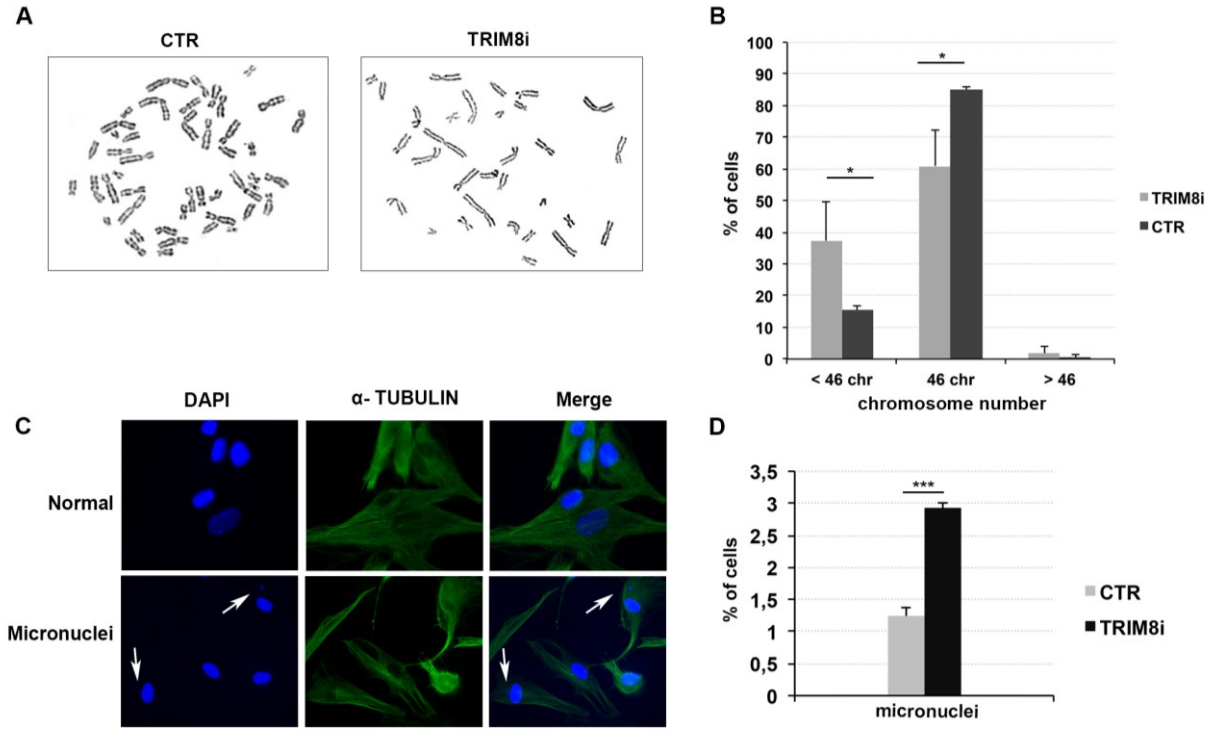

Figure 22. TRIM8 silencing causes chromosomal instability (A) After transfection with control siRNA and TRIM8 siRNA, metaphases of HF cells were prepared for karyotype analysis. Light microscopic images are shown for characteristic metaphase spread in a control (left) and a TRIM8-silenced cell (right). **(B)** Chromosome number distribution of CTR and TRIM8i cells are shown as percentages. For each experiment, 100 metaphase cells were analyzed in the control and TRIM8-silenced cell groups. Three independent experiments were performed, and error bars represent standard deviations. *, p<.05. **(C)** HF cells were transfected with control siRNA (CTR) and TRIM8 specific siRNAs (TRIM8i). Cells were stained for α -tubulin (green) and nucleus was stained with DAPI (blue) for immunofluorescence microscopy. Arrows indicate micronuclei. **(D)** Micronuclei number of CTR and TRIM8i cells are shown as percentages. For each experiment, 1200 cells were analyzed in control and TRIM8-silenced groups. Three independent experiments were performed, and error bars represent standard deviations. ***, p<.001.

5. DISCUSSION

In a research for TRIM8-related transcriptomic profile of embrionic neural stem cells (eNSC) we found 723 differentially expressed genes that significantly enriched 18 pathways related to cell-morphology, cell death and survival, with a preponderantly representation of signalling pathways related to neurotransmission and to CNS, including axonal guidance, GABA Receptor, ephrin B, synaptic long-term potentiation/depression, and glutamate receptor. Among these pathways we identified as a common gene, *M-RAS*, a member of the Ras family of the small GTPases. It functions as a signal transducer in multiple processes such as cell growth and differentiation. The dysregulation of RAS signaling plays a vital role in the oncogenesis of several cancers, including glioma[100, 101]. Interestingly, *MRAS* transcriptional activation is induced by unphosphorylated STAT3 and a strong correlation between *MRAS* and *STAT3* mRNA has been reported in many cancers including colon, stomach, ovary, lung, kidney, and rectum[102]. Moreover, two out of five CNS-related pathways, the glutamate receptor and synaptic long-term potentiation/depression signalling, share *GRM8*, *GRM1*, and *GRIA4* genes. These genes encode for glutamate receptors which are highly expressed in the mammalian brain and mediate important functions in cerebellar development, synaptic plasticity, neuroprotective and neurodegenerative mechanisms (GRM1 and GRM8)[103] and in fast synaptic excitatory neurotransmission (GRIA4)[104]. Interestingly, the JAK-STAT signaling pathway regulates these glutamate receptors expressions in the CNS in response to various cytokines, hormones, and growth factors[105, 106].

Finally, in a research of the most over-represented diseases and biological functions, we found as the most pleiotropic gene, *VEGF* that participate to 51 out of 68 biological functions and pathways. VEGFA is a member of the PDGF/VEGF growth factor family that plays multiple roles in the CNS by regulating neuronal migration, angiogenesis, and axonal path finding[107-109]. VEGFA is highly expressed in glioma. Glioma cells secrete VEGFA that binds the VEGFA receptor stimulating the tumor vascular endothelial cell proliferation, migration and tube-like structure formation, and finally promotes tumor neovascularization[109, 110]. In line with our findings, this axis is mediated by a number of signaling pathways including JAK-STAT[111, 112].

Furthermore, we validated the transcriptomic data, detecting a global deregulation of the JAK-STAT pathway in accordance to RNA-Seq data. Among a panel of genes involved in the JAK-STAT pathway, we found *Epor*, *Jak1*, and *Smad5* significantly down-regulated while *Stat3* up-regulated in embryonic neural stem cells overexpressing TRIM8. Of interest, all these four genes are implicated in glioma. STAT3 is a critical mediator of tumorigenesis, tumor progression, suppression of anti-tumor immunity in GB[113]. The pleiotropic Erythropoietin, EPO, and its receptor EPOR were aberrantly expressed in brain tumors and act as crucial factors in promoting

angiogenesis in human gliomas[111]. Finally, *JAK1* and *SMAD5* were recently found up-regulated in glioma cells[114, 115]. In addition, *SMAD5* was reported as a target gene of the miR-135 known to be down-regulated in GB cell lines. Forced expression of miR-135b into glioma stem cells markedly suppressed proliferation, motility and invasion of glioma cells as well as their stem cell-like phenotype through targeting *SMAD5*[116].

Overall these evidences demonstrate that *TRIM8* is a gene with specific functions in the central nervous system and in neurotransmission. In this cellular context, TRIM8 deregulates genes and entire pathways, like JAK-STAT pathway, involved in cancer and particularly in glioma progression. This evidence is further strengthened by our correlation and survival analysis between the transcriptional level of TRIM8 and these brain-related genes in a cohort of Low Grade Glioma (LGG) and Glioblastoma (GB) tissues from The Cancer Genome Atlas (TCGA) Research Network.

Our data analysis has revealed a number of pathways involving the JAK-STAT regulatory network, one of the most crucial signaling pathways implicated in the control of CNS functions by modulating the expression of genes linked to neurogenesis/gliogenesis, hormonal regulation, synaptic plasticity, and inflammation or tumorigenesis in response to hormones, growth factors or cytokines[117-119]. Consequently, dysregulation of the JAK-STAT pathway is at the heart of most brain disorders, including glioma, lesions, ischemia, neurodegenerative disorders, and epilepsies[120]. Moreover previous reports linked TRIM8 to the JAK-STAT signaling pathway. Experimental evidences highlighted the existence of a functional link between TRIM8 and STAT3 in several cellular contexts, including glioma stem cells[80, 81, 83]. In particular, TRIM8 activates STAT3 either by a directly negative proteosomal regulation of STAT3 inhibitor PIAS3 or modulating the translocation of phosphorylated STAT3 into the nucleus through the interaction with the Hsp90β[80, 81]. Interestingly, a recent study identifies *TRIM8* as potential oncogene in glioblastoma multiforme through its regulation of PIAS3-STAT3 loop[83]. As for many TRIM proteins, TRIM8 expression is induced by IFN that acts through the JAK-STAT signaling pathway inducing the transcription of a large set of JAK-targeted genes[69].

Starting with this evidences, we speculated that in the cytoplasmic fraction, TRIM8 physically interacts with STAT3 through the STAT3 Src homology 2 domain (SH2), that has been reported as linked to different tumors development[121]. In this cellular compartment the ectopic expression of TRIM8 may reinforce the capability of STAT3 to interact with JAK and to promote the proteosomal degradation of PIAS3 as already suggested by[80]. Consequently, these molecular events may accelerate the nuclear import of STAT3, accordingly to[81]. Thus, in line with our luciferase assays data, we speculated that TRIM8 increases STAT3 transcriptional activity probably promoting STAT3 accumulation in the nucleus with consequent binding of STAT3 to its responsive

sequences (SIE) on DNA. We have also shown that in the nucleus, TRIM8 binds STAT3 inducible elements (SIE) guessing that this could be another way by which TRIM8 enhances STAT3 transcriptional activity on a repertoire of brain disease and cancer-related genes, probably via nuclear factors (Fig. 23). STAT3 is a crucial convergence point of several major oncogenic signaling pathways, including those of EGFR, PDGFR, c-Met, IL-6R/ gp130, cytoplasmic enzymes in the JAK family, and the Src family of kinases[122], and this makes STAT3 an attractive molecular therapeutic target in GB. Thus, the identification of new regulators of STAT3 is crucial for novel therapeutic strategies.

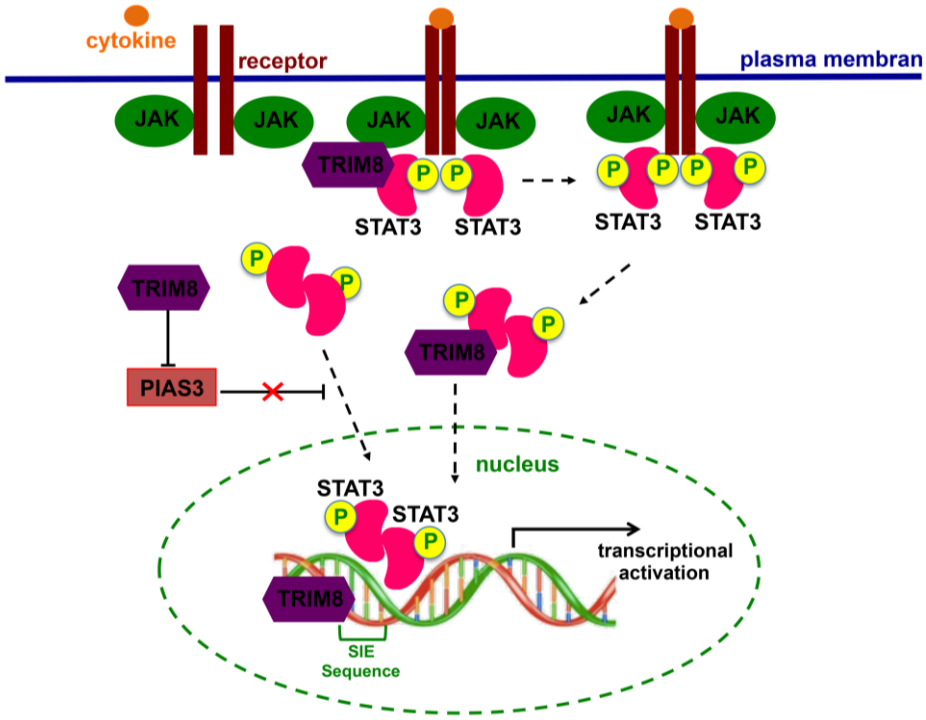

Figure 23. Schematic model of the TRIM8 and STAT3 binding to the STAT3-responsive element in the nucleus. The model suggests that in the cytoplasmic fraction, the ectopic expression of TRIM8 may, on the one hand strengthen the ability of STAT3 to interact with JAK and on the other promote the degradation of PIAS3 through proteosomal degradation. These molecular events result in enhanced STAT3 activation and nuclear translocation. In the nucleus TRIM8 may contribute to the recruitment of STAT3 to SIE elements of a repertoire of brain disease and cancer-related genes.

Many studies demonstrated the involvement of E3 ubiquitin ligase TRIM8 in the tumorigenic processes, including glioma[53, 54, 123], although the repertoire of its interactors and substrates has yet to be elucidated. In the second part of this study we identified TRIM8-interacting proteins in normal embryonic neural stem cells, giving experimental evidences that TRIM8 is a new component of the mitotic spindle machinery. Here, we identified several TRIM8 putative interactors using a functional proteomic approach based on TRIM8 immunoprecipitation assays coupled to LC-MS/MS identification of protein interactors. Proteomic data revealed that 22% of TRIM8 potential interactors are involved in the mitotic spindle machinery functions.

The mitotic machinery involves many critical factors and enzymes that need to be finely regulated to control the appropriate timing of events that lead to chromosome segregation and to prevent aneuploidy[124]. Many E3 ligases regulate cell cycle progression and mitosis, either directly by modulating the cell cycle check points and controlling key mitotic regulators, or indirectly by altering the functions of microtubule interacting proteins[87, 88, 124-126]. Among them, kinesins are motor proteins that move along microtubules usually carry cargo, such as organelles and vesicles from the center of a cell to its periphery[124, 127, 128]. Among the E3 ligases, many TRIM proteins are involved in the control of cell cycle transition phases and mitotic spindle formation. In particular, TRIM27, TRIM28, TRIM29, TRIM52, TRIM66 and TRIM68 led to cell cycle arrest when depleted or silenced[24, 71, 129-132]. TRIM proteins localize at centrosomes and spindle poles and are important in the maintenance of the genome stability, coordinating centrosomes duplication[32-36]. Other TRIMs like, TRIM17, TRIM36 and TRIM69 play a role in chromosome segregation and cell-cycle regulation interacting with and regulating proteolysis, and proteasome-dependent degradation of several kinetochore proteins[34, 133, 134].

Among the mitotic TRIM8 potential interactors, we confirmed the interaction with the mitotic proteins Haus1, Kif2c, KIF11 and KIFC1 kinesins, strongly suggesting a role of TRIM8 in the crucial mitotic process. HAUS1, primarily localized to the spindle during mitosis, is a regulator of spindle function and integrity and its silencing results in the destabilization of kinetochore microtubules and the eventual formation of multipolar spindles[135]. KIF2C is highly enriched at centrosomes, centromeres/kinetochores and at the spindle midzone during mitosis, where it efficiently regulates the microtubule dynamics and ensure proper chromosomes attachments to the spindle. Of interest, KIF2C was described as marker for prognosis in human gliomas[136]. Relevant for our work, KIF11 is a plus-end directed microtubule motor protein that drives bipolar spindle formation, while KIFC1 is a minus-end-directed motor protein which belongs to kinesin-14 motor proteins family; they utilize the chemical energy of ATP hydrolysis to move along microtubules from their minus- to their plus-end, and vice versa[38, 39, 41]. There is an antagonistic relationship between KIFC1 and KIF11 in order to crosslink and slide microtubules, a common mechanism to maintain correct spindle organization[41]. Thus, dysregulation of KIF11 or KIFC1 expression is responsible for an aberrant spindles phenotype[124, 137-139]. This imbalance can be determined by variation in the expression levels of both KIFC1 and KIF11, often correlated to different forms of cancer, including glioma[38, 48, 140].

Our functional studies showed that TRIM8 co-localizes with centrosomes and midbodies during mitosis, as showed for other TRIMs[32-35] and that TRIM8-silencing prevents the centrosome separation at the beginning of mitosis, leading to the monopolar spindle organization and to a delay

of mitosis progression in metaphase cells. Consequently, TRIM8 silencing resulted in chromosome instability-associated phenotypes, including aneuploidy cells and micronucleus formation. Given the biological functions of HAUS1, and KIF2C, KIF11 and KIFC1, we suggested that TRIM8, probably through its E3 ubiquitin ligase activity, might play a crucial role in the regulatory functions of the mitotic process through the regulation of the key mitotic factors. Aberrant expression of TRIM8 could result in an altered control of mitotic proteins functions with important consequences on mitotic dynamics and chromosome stability. This hypothesis is also supported by previous studies, which demonstrated that KIF11 inhibition and KIFC1 overexpression are sufficient to induce a monopolar spindle phenotype in mitotic cells[38, 124, 138], resembling the monopolar phenotype we observed in TRIM8-silenced cells. Accordingly, our data demonstrated that the monopolar spindle phenotype is most represented in the U87MG glioblastoma cells, compared to HeLa cells and Human Fibroblasts. This data closely links TRIM8 expression with the monopolar phenotype in glioma cells since, together with TRIM8 transiently silencing through shRNAs, TRIM8 expression itself is repressed in gliomas[53].

It has been previously shown that TRIM8 may play a role in cell cycle progression in cancer cell lines. In human osteosarcoma cell lines, TRIM8 physically interacts, stabilizes and activates p53 protein, resulting in a suppression of cell proliferation due to a p53-dependent cell cycle arrest in G1[54]. In our work, we demonstrated that silencing of TRIM8 induces a delay of the mitosis progression with a cell accumulation in G2/M in different cellular types, including U87MG glioblastoma cell lines, confirming a possible TRIM8 role in controlling cancer cells growth.

Although our evidences showed that TRIM8 silencing is associated with a monopolar spindle formation and a delay in the progression of mitosis, TRIM8i cells are still capable to proliferate, suggesting that TRIM8-induced mitotic defect could be a transient phenotype. Although a number of reasonable explanations are possible, we hypothesized that the transient nature of shRNAs may contribute to escape the delay of the mitotic progression, or that silenced cells somehow escape the mitotic checkpoint, which is essential to maintain mitotic fidelity[141].

6. CONCLUSIONS

The first part of this study provides novel insights on the physiological TRIM8 function by profiling for the first time the primary Neural Stem Cell over-expressing TRIM8 by using RNA-Sequencing methodology, substantiating the role of TRIM8 in the brain functions through the dysregulation of genes involved in different CNS-related pathways, including JAK-STAT.

Moreover, in the second part of the present study we provided insights on the physiological function of TRIM8 in mitotic machinery and pointed to an emerging role for TRIM8 in brain-related phenotypes, with relevant implication for gliomagenesis. However, further analysis will be needed to elucidate the functional TRIM8-key mitotic factors interaction and the molecular mechanism by which TRIM8 is involved in this intriguing process and its impact on the brain-related cancers.

7. BIBLIOGRAPHY

1. H. G. Wirsching, E. Galanis, M. Weller, Glioblastoma. *Handb Clin Neurol* **134**, 381-397 (2016).
2. A. F. Tamimi, M. Juweid, in *Glioblastoma,* S. De Vleeschouwer, Ed. (Brisbane (AU), 2017).
3. B. Vastrad, C. Vastrad, A. Godavarthi, R. Chandrashekar, Molecular mechanisms underlying gliomas and glioblastoma pathogenesis revealed by bioinformatics analysis of microarray data. *Med Oncol* **34**, 182 (2017).
4. B. A. Reddy, L. D. Etkin, P. S. Freemont, A novel zinc finger coiled-coil domain in a family of nuclear proteins. *Trends Biochem Sci* **17**, 344-345 (1992).
5. K. L. Borden, RING fingers and B-boxes: zinc-binding protein-protein interaction domains. *Biochem Cell Biol* **76**, 351-358 (1998).
6. A. Reymond *et al.*, The tripartite motif family identifies cell compartments. *EMBO J* **20**, 2140-2151 (2001).
7. X. Li, J. Sodroski, The TRIM5alpha B-box 2 domain promotes cooperative binding to the retroviral capsid by mediating higher-order self-association. *J Virol* **82**, 11495-11502 (2008).
8. L. Micale, E. Chaignat, C. Fusco, A. Reymond, G. Merla, The tripartite motif: structure and function. *Adv Exp Med Biol* **770**, 11-25 (2012).
9. M. A. Massiah *et al.*, Solution structure of the MID1 B-box2 CHC(D/C)C(2)H(2) zinc-binding domain: insights into an evolutionarily conserved RING fold. *J Mol Biol* **369**, 1-10 (2007).
10. S. Hatakeyama, TRIM Family Proteins: Roles in Autophagy, Immunity, and Carcinogenesis. *Trends Biochem Sci* **42**, 297-311 (2017).
11. G. Meroni, G. Diez-Roux, TRIM/RBCC, a novel class of 'single protein RING finger' E3 ubiquitin ligases. *Bioessays* **27**, 1147-1157 (2005).
12. A. Hershko, A. Ciechanover, The ubiquitin system. *Annu Rev Biochem* **67**, 425-479 (1998).
13. W. Zaky *et al.*, The ubiquitin-proteasome pathway in adult and pediatric brain tumors: biological insights and therapeutic opportunities. *Cancer Metastasis Rev* **36**, 617-633 (2017).
14. P. J. Vlachostergios, I. A. Voutsadakis, C. N. Papandreou, The ubiquitin-proteasome system in glioma cell cycle control. *Cell Div* **7**, 18 (2012).
15. R. Yau, M. Rape, The increasing complexity of the ubiquitin code. *Nat Cell Biol* **18**, 579-586 (2016).
16. L. Buetow, D. T. Huang, Structural insights into the catalysis and regulation of E3 ubiquitin ligases. *Nat Rev Mol Cell Biol* **17**, 626-642 (2016).
17. L. J. Crawford, C. K. Johnston, A. E. Irvine, TRIM proteins in blood cancers. *J Cell Commun Signal* **12**, 21-29 (2018).
18. S. Hatakeyama, TRIM proteins and cancer. *Nat Rev Cancer* **11**, 792-804 (2011).
19. A. M. Weissman, Regulating protein degradation by ubiquitination. *Immunol Today* **18**, 189-198 (1997).
20. S. L. Tang, Y. L. Gao, H. Wen-Zhong, Knockdown of TRIM37 suppresses the proliferation, migration and invasion of glioma cells through the inactivation of PI3K/Akt signaling pathway. *Biomed Pharmacother* **99**, 59-64 (2018).
21. Y. Zhang *et al.*, A novel PI3K/AKT signaling axis mediates Nectin-4-induced gallbladder cancer cell proliferation, metastasis and tumor growth. *Cancer Lett* **375**, 179-189 (2016).
22. L. H. Zhang *et al.*, TRIM24 promotes glioma progression and enhances chemoresistance through activation of the PI3K/Akt signaling pathway. *Oncogene* **34**, 600-610 (2015).
23. D. Lv *et al.*, TRIM24 is an oncogenic transcriptional co-activator of STAT3 in glioblastoma. *Nat Commun* **8**, 1454 (2017).
24. Z. X. Qi *et al.*, TRIM28 as an independent prognostic marker plays critical roles in glioma progression. *J Neurooncol* **126**, 19-26 (2016).
25. I. Jovcevska *et al.*, TRIM28 and beta-actin identified via nanobody-based reverse proteomics approach as possible human glioblastoma biomarkers. *PLoS One* **9**, e113688 (2014).

26. K. Di, M. E. Linskey, D. A. Bota, TRIM11 is overexpressed in high-grade gliomas and promotes proliferation, invasion, migration and glial tumor growth. *Oncogene* **32**, 5038-5047 (2013).
27. J. L. Boulay *et al.*, Loss of heterozygosity of TRIM3 in malignant gliomas. *BMC Cancer* **9**, 71 (2009).
28. J. Zhang *et al.*, TRIM45 functions as a tumor suppressor in the brain via its E3 ligase activity by stabilizing p53 through K63-linked ubiquitination. *Cell Death Dis* **8**, e2831 (2017).
29. S. Fournane, K. Krupina, C. Kleiss, I. Sumara, Decoding ubiquitin for mitosis. *Genes Cancer* **3**, 697-711 (2012).
30. W. Zhan *et al.*, TRIM59 Promotes the Proliferation and Migration of Non-Small Cell Lung Cancer Cells by Upregulating Cell Cycle Related Proteins. *PLoS One* **10**, e0142596 (2015).
31. K. M. Short, T. C. Cox, Subclassification of the RBCC/TRIM superfamily reveals a novel motif necessary for microtubule binding. *J Biol Chem* **281**, 8970-8980 (2006).
32. Z. X. Xu, W. X. Zou, P. Lin, K. S. Chang, A role for PML3 in centrosome duplication and genome stability. *Mol Cell* **17**, 721-732 (2005).
33. J. Petersson *et al.*, The human IFN-inducible p53 target gene TRIM22 colocalizes with the centrosome independently of cell cycle phase. *Exp Cell Res* **316**, 568-579 (2010).
34. R. Sinnott *et al.*, Mechanisms promoting escape from mitotic stress-induced tumor cell death. *Cancer Res* **74**, 3857-3869 (2014).
35. S. H. Neo *et al.*, TRIM28 Is an E3 Ligase for ARF-Mediated NPM1/B23 SUMOylation That Represses Centrosome Amplification. *Mol Cell Biol* **35**, 2851-2863 (2015).
36. H. Izumi, Y. Kaneko, Trim32 facilitates degradation of MYCN on spindle poles and induces asymmetric cell division in human neuroblastoma cells. *Cancer Res* **74**, 5620-5630 (2014).
37. M. A. Mandell *et al.*, Correction: TRIM17 contributes to autophagy of midbodies while actively sparing other targets from degradation. *J Cell Sci* **130**, 1194 (2017).
38. Y. Asbaghi, L. L. Thompson, Z. Lichtensztejn, K. J. McManus, KIF11 silencing and inhibition induces chromosome instability that may contribute to cancer. *Genes Chromosomes Cancer* **56**, 668-680 (2017).
39. B. J. Mann, P. Wadsworth, Distribution of Eg5 and TPX2 in mitosis: Insight from CRISPR tagged cells. *Cytoskeleton (Hoboken)* **75**, 508-521 (2018).
40. J. S. Weinger, M. Qiu, G. Yang, T. M. Kapoor, A nonmotor microtubule binding site in kinesin-5 is required for filament crosslinking and sliding. *Curr Biol* **21**, 154-160 (2011).
41. Z. Y. She, W. X. Yang, Molecular mechanisms of kinesin-14 motors in spindle assembly and chromosome segregation. *J Cell Sci* **130**, 2097-2110 (2017).
42. C. T. Friel, J. Howard, Coupling of kinesin ATP turnover to translocation and microtubule regulation: one engine, many machines. *J Muscle Res Cell Motil* **33**, 377-383 (2012).
43. C. E. Walczak, S. Verma, T. J. Mitchison, XCTK2: a kinesin-related protein that promotes mitotic spindle assembly in Xenopus laevis egg extracts. *J Cell Biol* **136**, 859-870 (1997).
44. I. Brust-Mascher, J. M. Scholey, Mitotic motors and chromosome segregation: the mechanism of anaphase B. *Biochem Soc Trans* **39**, 1149-1153 (2011).
45. V. Mountain *et al.*, The kinesin-related protein, HSET, opposes the activity of Eg5 and cross-links microtubules in the mammalian mitotic spindle. *J Cell Biol* **147**, 351-366 (1999).
46. D. J. Sharp, G. C. Rogers, J. M. Scholey, Cytoplasmic dynein is required for poleward chromosome movement during mitosis in Drosophila embryos. *Nat Cell Biol* **2**, 922-930 (2000).
47. M. Yukawa, C. Ikebe, T. Toda, The Msd1-Wdr8-Pkl1 complex anchors microtubule minus ends to fission yeast spindle pole bodies. *J Cell Biol* **209**, 549-562 (2015).
48. Q. Xiao, X. Hu, Z. Wei, K. Y. Tam, Cytoskeleton Molecular Motors: Structures and Their Functions in Neuron. *Int J Biol Sci* **12**, 1083-1092 (2016).
49. N. C. Baudoin, D. Cimini, A guide to classifying mitotic stages and mitotic defects in fixed cells. *Chromosoma* **127**, 215-227 (2018).

50. M. F. Caratozzolo, F. Marzano, F. Mastropasqua, E. Sbisa, A. Tullo, TRIM8: Making the Right Decision between the Oncogene and Tumour Suppressor Role. *Genes (Basel)* **8**, (2017).
51. F. Carinci *et al.*, Molecular classification of nodal metastasis in primary larynx squamous cell carcinoma. *Transl Res* **150**, 233-245 (2007).
52. S. R. Vincent, D. A. Kwasnicka, P. Fretier, A novel RING finger-B box-coiled-coil protein, GERP. *Biochem Biophys Res Commun* **279**, 482-486 (2000).
53. L. Micale *et al.*, TRIM8 downregulation in glioma affects cell proliferation and it is associated with patients survival. *BMC Cancer* **15**, 470 (2015).
54. M. F. Caratozzolo *et al.*, TRIM8 modulates p53 activity to dictate cell cycle arrest. *Cell Cycle* **11**, 511-523 (2012).
55. M. F. Caratozzolo *et al.*, TRIM8 anti-proliferative action against chemo-resistant renal cell carcinoma. *Oncotarget* **5**, 7446-7457 (2014).
56. M. H. Park, J. T. Hong, Roles of NF-kappaB in Cancer and Inflammatory Diseases and Their Therapeutic Approaches. *Cells* **5**, (2016).
57. M. Karin, NF-kappaB as a critical link between inflammation and cancer. *Cold Spring Harb Perspect Biol* **1**, a000141 (2009).
58. M. S. Hayden, S. Ghosh, NF-kappaB in immunobiology. *Cell Res* **21**, 223-244 (2011).
59. S. Liu, Z. J. Chen, Expanding role of ubiquitination in NF-kappaB signaling. *Cell Res* **21**, 6-21 (2011).
60. C. Behrends, J. W. Harper, Constructing and decoding unconventional ubiquitin chains. *Nat Struct Mol Biol* **18**, 520-528 (2011).
61. V. Baud, E. Derudder, Control of NF-kappaB activity by proteolysis. *Curr Top Microbiol Immunol* **349**, 97-114 (2011).
62. Q. Li *et al.*, Tripartite motif 8 (TRIM8) modulates TNFalpha- and IL-1beta-triggered NF-kappaB activation by targeting TAK1 for K63-linked polyubiquitination. *Proc Natl Acad Sci U S A* **108**, 19341-19346 (2011).
63. D. Tomar *et al.*, Nucleo-cytoplasmic trafficking of TRIM8, a novel oncogene, is involved in positive regulation of TNF induced NF-kappaB pathway. *PLoS One* **7**, e48662 (2012).
64. S. Vallabhapurapu, M. Karin, Regulation and function of NF-kappaB transcription factors in the immune system. *Annu Rev Immunol* **27**, 693-733 (2009).
65. A. Sorrentino *et al.*, The type I TGF-beta receptor engages TRAF6 to activate TAK1 in a receptor kinase-independent manner. *Nat Cell Biol* **10**, 1199-1207 (2008).
66. Y. H. Fan *et al.*, USP4 targets TAK1 to downregulate TNFalpha-induced NF-kappaB activation. *Cell Death Differ* **18**, 1547-1560 (2011).
67. H. D. Jang, K. Yoon, Y. J. Shin, J. Kim, S. Y. Lee, PIAS3 suppresses NF-kappaB-mediated transcription by interacting with the p65/RelA subunit. *J Biol Chem* **279**, 24873-24880 (2004).
68. Y. Wu, B. P. Zhou, TNF-alpha/NF-kappaB/Snail pathway in cancer cell migration and invasion. *Br J Cancer* **102**, 639-644 (2010).
69. E. Toniato *et al.*, TRIM8/GERP RING finger protein interacts with SOCS-1. *J Biol Chem* **277**, 37315-37322 (2002).
70. J. Pencik *et al.*, JAK-STAT signaling in cancer: From cytokines to non-coding genome. *Cytokine* **87**, 26-36 (2016).
71. P. H. Chen, H. Yao, L. J. Huang, Cytokine Receptor Endocytosis: New Kinase Activity-Dependent and -Independent Roles of PI3K. *Front Endocrinol (Lausanne)* **8**, 78 (2017).
72. J. G. Zhang *et al.*, The conserved SOCS box motif in suppressors of cytokine signaling binds to elongins B and C and may couple bound proteins to proteasomal degradation. *Proc Natl Acad Sci U S A* **96**, 2071-2076 (1999).
73. Y. Shi *et al.*, Roles of STAT3 in leukemia (Review). *Int J Oncol* **53**, 7-20 (2018).
74. A. T. Namanja, J. Wang, R. Buettner, L. Colson, Y. Chen, Allosteric Communication across STAT3 Domains Associated with STAT3 Function and Disease-Causing Mutation. *J Mol Biol* **428**, 579-589 (2016).

75. H. Yu, M. Kortylewski, D. Pardoll, Crosstalk between cancer and immune cells: role of STAT3 in the tumour microenvironment. *Nat Rev Immunol* **7**, 41-51 (2007).
76. H. Guo *et al.*, Vascular endothelial growth factor: an attractive target in the treatment of hypoxic/ischemic brain injury. *Neural Regen Res* **11**, 174-179 (2016).
77. B. Groner, P. Lucks, C. Borghouts, The function of Stat3 in tumor cells and their microenvironment. *Semin Cell Dev Biol* **19**, 341-350 (2008).
78. K. Shuai, Regulation of cytokine signaling pathways by PIAS proteins. *Cell Res* **16**, 196-202 (2006).
79. S. Huang, Regulation of metastases by signal transducer and activator of transcription 3 signaling pathway: clinical implications. *Clin Cancer Res* **13**, 1362-1366 (2007).
80. F. Okumura, Y. Matsunaga, Y. Katayama, K. I. Nakayama, S. Hatakeyama, TRIM8 modulates STAT3 activity through negative regulation of PIAS3. *J Cell Sci* **123**, 2238-2245 (2010).
81. F. Okumura, A. J. Okumura, M. Matsumoto, K. I. Nakayama, S. Hatakeyama, TRIM8 regulates Nanog via Hsp90beta-mediated nuclear translocation of STAT3 in embryonic stem cells. *Biochim Biophys Acta* **1813**, 1784-1792 (2011).
82. M. M. Setati *et al.*, Leukemia inhibitory factor promotes Hsp90 association with STAT3 in mouse embryonic stem cells. *IUBMB Life* **62**, 61-66 (2010).
83. C. Zhang *et al.*, TRIM8 regulates stemness in glioblastoma through PIAS3-STAT3. *Mol Oncol* **11**, 280-294 (2017).
84. S. Penuelas *et al.*, TGF-beta increases glioma-initiating cell self-renewal through the induction of LIF in human glioblastoma. *Cancer Cell* **15**, 315-327 (2009).
85. H. Wang *et al.*, Targeting interleukin 6 signaling suppresses glioma stem cell survival and tumor growth. *Stem Cells* **27**, 2393-2404 (2009).
86. R. F. Shearer, M. Iconomou, C. K. Watts, D. N. Saunders, Functional Roles of the E3 Ubiquitin Ligase UBR5 in Cancer. *Mol Cancer Res* **13**, 1523-1532 (2015).
87. A. Mani, E. P. Gelmann, The ubiquitin-proteasome pathway and its role in cancer. *J Clin Oncol* **23**, 4776-4789 (2005).
88. K. I. Nakayama, K. Nakayama, Ubiquitin ligases: cell-cycle control and cancer. *Nat Rev Cancer* **6**, 369-381 (2006).
89. H. Zong, L. F. Parada, S. J. Baker, Cell of origin for malignant gliomas and its implication in therapeutic development. *Cold Spring Harb Perspect Biol* **7**, (2015).
90. F. H. Gage, S. Temple, Neural stem cells: generating and regenerating the brain. *Neuron* **80**, 588-601 (2013).
91. M. Terrile *et al.*, PDGF-B-driven gliomagenesis can occur in the absence of the proteoglycan NG2. *BMC Cancer* **10**, 550 (2010).
92. A. M. Bolger, M. Lohse, B. Usadel, Trimmomatic: a flexible trimmer for Illumina sequence data. *Bioinformatics* **30**, 2114-2120 (2014).
93. O. Palmieri *et al.*, Gene expression of muscular and neuronal pathways is cooperatively dysregulated in patients with idiopathic achalasia. *Sci Rep* **6**, 31549 (2016).
94. S. Rozen, H. Skaletsky, Primer3 on the WWW for general users and for biologist programmers. *Methods Mol Biol* **132**, 365-386 (2000).
95. L. Micale *et al.*, A fish-specific transposable element shapes the repertoire of p53 target genes in zebrafish. *PLoS One* **7**, e46642 (2012).
96. V. Pisa *et al.*, The molecular chaperone Hsp90 is a component of the cap-binding complex and interacts with the translational repressor Cup during Drosophila oogenesis. *Gene* **432**, 67-74 (2009).
97. G. Huang, H. Yan, S. Ye, C. Tong, Q. L. Ying, STAT3 phosphorylation at tyrosine 705 and serine 727 differentially regulates mouse ESC fates. *Stem Cells* **32**, 1149-1160 (2014).
98. Y. Sekine *et al.*, Leukemia inhibitory factor-induced phosphorylation of STAP-2 on tyrosine-250 is involved in its STAT3-enhancing activity. *Biochem Biophys Res Commun* **356**, 517-522 (2007).

99. D. Cimini, D. Fioravanti, E. D. Salmon, F. Degrassi, Merotelic kinetochore orientation versus chromosome mono-orientation in the origin of lagging chromosomes in human primary cells. *J Cell Sci* **115**, 507-515 (2002).
100. E. C. Holland *et al.*, Combined activation of Ras and Akt in neural progenitors induces glioblastoma formation in mice. *Nat Genet* **25**, 55-57 (2000).
101. L. Santarpia, S. M. Lippman, A. K. El-Naggar, Targeting the MAPK-RAS-RAF signaling pathway in cancer therapy. *Expert Opin Ther Targets* **16**, 103-119 (2012).
102. J. Yang *et al.*, Novel roles of unphosphorylated STAT3 in oncogenesis and transcriptional regulation. *Cancer Res* **65**, 939-947 (2005).
103. M. G. Baudry, R.; Pernot, F.; Bouteiller, J.; Bi, X. , Roles of group I metabotropic glutamate receptors under physiological conditions and in neurodegeneration. *Membr. Transp. Signal.* **1**, 523–532 (2012).
104. M. L. MacDonald *et al.*, Altered glutamate protein co-expression network topology linked to spine loss in the auditory cortex of schizophrenia. *Biol Psychiatry* **77**, 959-968 (2015).
105. I. V. Lund *et al.*, BDNF selectively regulates GABAA receptor transcription by activation of the JAK/STAT pathway. *Sci Signal* **1**, ra9 (2008).
106. D. I. Orellana, R. A. Quintanilla, C. Gonzalez-Billault, R. B. Maccioni, Role of the JAKs/STATs pathway in the intracellular calcium changes induced by interleukin-6 in hippocampal neurons. *Neurotox Res* **8**, 295-304 (2005).
107. F. Mackenzie, C. Ruhrberg, Diverse roles for VEGF-A in the nervous system. *Development* **139**, 1371-1380 (2012).
108. A. Quaegebeur, C. Lange, P. Carmeliet, The neurovascular link in health and disease: molecular mechanisms and therapeutic implications. *Neuron* **71**, 406-424 (2011).
109. H. K. Yang *et al.*, Downregulation of LRIG2 expression inhibits angiogenesis of glioma via EGFR/VEGF-A pathway. *Oncol Lett* **14**, 4021-4028 (2017).
110. D. A. Reardon *et al.*, A review of VEGF/VEGFR-targeted therapeutics for recurrent glioblastoma. *J Natl Compr Canc Netw* **9**, 414-427 (2011).
111. B. Nico *et al.*, Epo is involved in angiogenesis in human glioma. *J Neurooncol* **102**, 51-58 (2011).
112. J. B. Casaletto, A. I. McClatchey, Spatial regulation of receptor tyrosine kinases in development and cancer. *Nat Rev Cancer* **12**, 387-400 (2012).
113. K. Swiatek-Machado, B. Kaminska, STAT signaling in glioma cells. *Adv Exp Med Biol* **986**, 189-208 (2013).
114. C. Du *et al.*, Microarray data analysis to identify crucial genes regulated by CEBPB in human SNB19 glioma cells. *World J Surg Oncol* **14**, 258 (2016).
115. D. A. Almiron Bonnin *et al.*, Secretion-mediated STAT3 activation promotes self-renewal of glioma stem-like cells during hypoxia. *Oncogene* **37**, 1107-1118 (2018).
116. V. Lulli *et al.*, miR-135b suppresses tumorigenesis in glioblastoma stem-like cells impairing proliferation, migration and self-renewal. *Oncotarget* **6**, 37241-37256 (2015).
117. C. S. Nicolas *et al.*, The role of JAK-STAT signaling within the CNS. *JAKSTAT* **2**, e22925 (2013).
118. C. S. Nicolas *et al.*, The Jak/STAT pathway is involved in synaptic plasticity. *Neuron* **73**, 374-390 (2012).
119. H. Qin *et al.*, Inhibition of the JAK/STAT Pathway Protects Against alpha-Synuclein-Induced Neuroinflammation and Dopaminergic Neurodegeneration. *J Neurosci* **36**, 5144-5159 (2016).
120. H. L. Grabenstatter *et al.*, The effect of STAT3 inhibition on status epilepticus and subsequent spontaneous seizures in the pilocarpine model of acquired epilepsy. *Neurobiol Dis* **62**, 73-85 (2014).
121. T. T. Huang, J. C. Su, C. Y. Liu, C. W. Shiau, K. F. Chen, Alteration of SHP-1/p-STAT3 Signaling: A Potential Target for Anticancer Therapy. *Int J Mol Sci* **18**, (2017).

122. T. Bowman *et al.*, Stat3-mediated Myc expression is required for Src transformation and PDGF-induced mitogenesis. *Proc Natl Acad Sci U S A* **98**, 7319-7324 (2001).
123. F. Mastropasqua *et al.*, TRIM8 restores p53 tumour suppressor function by blunting N-MYC activity in chemo-resistant tumours. *Mol Cancer* **16**, 67 (2017).
124. S. A. Singh *et al.*, Co-regulation proteomics reveals substrates and mechanisms of APC/C-dependent degradation. *EMBO J* **33**, 385-399 (2014).
125. A. Ciechanover, A. L. Schwartz, The ubiquitin system: pathogenesis of human diseases and drug targeting. *Biochim Biophys Acta* **1695**, 3-17 (2004).
126. S. Sivakumar, G. J. Gorbsky, Spatiotemporal regulation of the anaphase-promoting complex in mitosis. *Nat Rev Mol Cell Biol* **16**, 82-94 (2015).
127. Y. Duan *et al.*, Ubiquitin ligase RNF20/40 facilitates spindle assembly and promotes breast carcinogenesis through stabilizing motor protein Eg5. *Nat Commun* **7**, 12648 (2016).
128. D. Labonte *et al.*, TRIM3 regulates the motility of the kinesin motor protein KIF21B. *PLoS One* **8**, e75603 (2013).
129. Y. Zhang *et al.*, TRIM27 functions as an oncogene by activating epithelial-mesenchymal transition and p-AKT in colorectal cancer. *Int J Oncol* **53**, 620-632 (2018).
130. W. Xu *et al.*, RNA interference against TRIM29 inhibits migration and invasion of colorectal cancer cells. *Oncol Rep* **36**, 1411-1418 (2016).
131. S. Benke *et al.*, Human tripartite motif protein 52 is required for cell context-dependent proliferation. *Oncotarget* **9**, 13565-13581 (2018).
132. Z. Tan *et al.*, Lentivirus-mediated RNA interference of tripartite motif 68 inhibits the proliferation of colorectal cancer cell lines SW1116 and HCT116 in vitro. *Oncol Lett* **13**, 2649-2655 (2017).
133. H. Endo, K. Ikeda, T. Urano, K. Horie-Inoue, S. Inoue, Terf/TRIM17 stimulates degradation of kinetochore protein ZWINT and regulates cell proliferation. *J Biochem* **151**, 139-144 (2012).
134. N. Miyajima, S. Maruyama, K. Nonomura, S. Hatakeyama, TRIM36 interacts with the kinetochore protein CENP-H and delays cell cycle progression. *Biochem Biophys Res Commun* **381**, 383-387 (2009).
135. S. Lawo *et al.*, HAUS, the 8-subunit human Augmin complex, regulates centrosome and spindle integrity. *Curr Biol* **19**, 816-826 (2009).
136. M. Sanhaji, C. T. Friel, L. Wordeman, F. Louwen, J. Yuan, Mitotic centromere-associated kinesin (MCAK): a potential cancer drug target. *Oncotarget* **2**, 935-947 (2011).
137. V. Sarli, A. Giannis, Targeting the kinesin spindle protein: basic principles and clinical implications. *Clin Cancer Res* **14**, 7583-7587 (2008).
138. A. Stolz, N. Ertych, H. Bastians, A phenotypic screen identifies microtubule plus end assembly regulators that can function in mitotic spindle orientation. *Cell Cycle* **14**, 827-837 (2015).
139. C. Zhu *et al.*, Functional analysis of human microtubule-based motor proteins, the kinesins and dyneins, in mitosis/cytokinesis using RNA interference. *Mol Biol Cell* **16**, 3187-3199 (2005).
140. M. Venere *et al.*, The mitotic kinesin KIF11 is a driver of invasion, proliferation, and self-renewal in glioblastoma. *Sci Transl Med* **7**, 304ra143 (2015).
141. A. Musacchio, E. D. Salmon, The spindle-assembly checkpoint in space and time. *Nat Rev Mol Cell Biol* **8**, 379-393 (2007).